Tectonics®

RESEARCH ARTICLE
10.1029/2023TC008189

Key Points:

- Detailed structural analysis is combined with three thermochronological methods to reconstruct low temperature deformation events
- K/Ar age of fault gouges date the fault activity directly, while apatite fission-track and (U-Th)/He data constrain the exhumation history
- The Maastrichtian age of the Nekézseny Thrust is interpreted in lights of the late-stage Alpine-Carpathian-Dinaric tectonic evolution

Correspondence to:
É. Oravecz,
orav.eva@gmail.com

Citation:
Oravecz, É., Benkó, Z., Arató, R., Dunkl, I., Héja, G., Kövér, S., et al. (2024). Age, kinematic and thermal constraints of syn-orogenic low-temperature deformation events: Insights from thermochronology and structural data of the Nekézseny Thrust (Alpine-Carpathian-Dinaric area). *Tectonics*, *43*, e2023TC008189. https://doi.org/10.1029/2023TC008189

Received 14 NOV 2023
Accepted 17 MAR 2024

Age, Kinematic and Thermal Constraints of Syn-Orogenic Low-Temperature Deformation Events: Insights From Thermochronology and Structural Data of the Nekézseny Thrust (Alpine-Carpathian-Dinaric Area)

Éva Oravecz[1], Zsolt Benkó[2,3], Róbert Arató[2,4], István Dunkl[4], Gábor Héja[5], Szilvia Kövér[1,6], Tibor Németh[7], and László Fodor[1,6]

[1]Department of Physical and Applied Geology, Institute of Geography and Earth Sciences, Eötvös Loránd University, Budapest, Hungary, [2]Institute of Nuclear Research of the Hungarian Academy of Sciences, Debrecen, Hungary, [3]Department of Mineralogy and Geology, Institute of Earth Sciences, University of Debrecen, Debrecen, Hungary, [4]Department of Sedimentology and Environmental Geology, Geoscience Center, University of Göttingen, Göttingen, Germany, [5]Supervisory Authority of Regulatory Affairs, Budapest, Hungary, [6]Hungarian Research Network, Institute of Earth Physics and Space Science, Sopron, Hungary, [7]Department of Geology and Meteorology, Institute of Geography and Earth Sciences, University of Pécs, Pécs, Hungary

Abstract Unraveling the age and kinematics of low temperature deformation events is crucial in understanding the late-stage evolution of orogens. However, accurate age constraints can often be challenging to obtain due to unideal outcrop conditions, large sedimentary hiatuses or the lack of well-defined thermal events. In this study, we show on the example of the Nekézseny Thrust, a poorly exposed late orogenic thrust in the southern Western Carpathians, that a combined approach of structural analysis and multi-method thermochronology can provide the necessary temporal, kinematic and thermal constraints for a detailed reconstruction of the deformation history. While structural mapping revealed that the Late Cretaceous Uppony Gosau Basin in the footwall of the Nekézseny Thrust underwent a significant post-Campanian and pre-Miocene shortening, K/Ar dating of fault gouge samples from the main fault zone constrained the primary thrusting event to the Maastrichtian. Based on the acquired apatite fission-track and (U-Th)/He ages, subsequent heating of the Upper Cretaceous sediments due to tectonic burial was limited to 75–100°C, followed by deformation-related and gradual cooling between the Eocene and Early Miocene. Considering the reconstructed deformation history, as well as the large-scale tectonic affinity of the displaced units in its footwall and hanging wall, the Nekézseny Thrust is a far-traveled (ca. 600 km) segment of the Late Cretaceous Alps-Dinarides contact zone, whose development was linked to the switch from lower plate to upper plate position with respect to the Sava Zone and Alpine Tethys sutures, respectively.

1. Introduction

The late-stage evolution of orogens is generally characterized by low-temperature deformation events, including continued syn- to post-orogenic thrusting and/or extensional collapse, which corresponds to the formation of brittle structures in the uppermost few kilometers of the crust (e.g., Folguera et al., 2015; Jia et al., 2020; Kahn et al., 2020). Constraining the temporal and thermal evolution along with the kinematics of these structures is essential to accurately reconstruct the more recent deformation history of orogens. However, it is particularly challenging to acquire reliable age constraints on such processes, as they are usually not characterized by well-defined thermal spikes, but rather a series of events close to the lower sensitivity limit of low temperature thermochornometers (Reiners et al., 2003).

The most straightforward option for dating low temperature events is to study syn-tectonic features and well-known stratigraphic markers in the deformed successions. For instance, growth strata allow for direct dating of fault movements and fold growth, whereas unconformities and stratigraphic units sealing the structures may constrain the deformation to a narrow time interval (e.g., Carrera & Munoz, 2008; DeCelles et al., 1995; Ortner, 2001; Suppe et al., 1992; Vergés et al., 2002), given that the age of the involved units is known. However, high resolution dating of formations is not always available, for instance, in the absence of routinely datable fossils/minerals or due to large sedimentary hiatuses, while limited outcrop conditions or the lack of subsurface

data may also prevent the accurate reconstruction of the deformation history. In such cases, low temperature thermochronology may provide alternative tools to acquire temporal constraints for the deformation.

In this study, we investigate the deformation history of the Nekézseny Thrust, a poorly exposed low-angle fault in the southernmost part of the Western Carpathians that bounds the Upper Cretaceous syn-orogenic sediments of the so-called Uppony Gosau Basin (Pelikán et al., 2005; Schréter, 1953). Similar deformed, dominantly siliciclastic successions, commonly referred to Gosau-type sediments (Hók et al., 2022; Kázmér et al., 2003; Ortner, 2001; Tari & Linzer, 2018; Wagreich, 1995; Wagreich & Faupl, 1994; Willingshofer et al., 1999), are known throughout the Alpine-Carpathian-Dinaric orogenic belt, and they may record both syn-orogenic flexural subsidence in front of emerging thrust sheets (Lužar-Oberiter et al., 2012; Matenco & Radivojević, 2012; Tari, 1995; Tari & Linzer, 2018) and/or orogen-parallel extension during the Late Cretaceous to Paleogene (Fügenschuh et al., 2000; Krohe, 1987; Madarás et al., 1996; Neubauer et al., 1995; Plašienka & Soták, 2015; Ratschbacher et al., 1989; Wagreich & Decker, 2001). Here, we combine detailed structural analysis with multi-method thermochronology to overcome the challenges resulting from the poor outcrop conditions and large sedimentary hiatuses. This combines approach allows to constrain the age and kinematics of the fault movements along the Nekézseny Thrust and to understand the tectono-thermal evolution of the Uppony Gosau Basin in its footwall. In absence of any noteworthy stratigraphic constraints, K/Ar dating of syn-kinematic fault gouges provided the only direct time constraints for the primary thrusting event, whereas low temperature thermochronology (apatite fission-track and (U-Th)/He dating) applied on Upper Cretaceous sandstone samples revealed insights from the deformation-related thermal evolution. As such, our study sheds light on a tectonically very intensive, but so far only vaguely understood time interval of the region.

2. Geological Background

The Alpine-Carpathian-Dinaric orogen and a series of corresponding foreland and back-arc basins (including the Pannonian Basin) formed during the Late Jurassic to Miocene closure of the Neotethys and Alpine Tethys oceanic domains (Handy et al., 2015; Schmid et al., 2020). The basement of the Pannonian Basin consists of two main tectonic units with different paleogeographic affinity and deformation history (Balla, 1983, 1986; Csontos et al., 1992; Kovács, 1982, 1984; Schmid et al., 2008, 2020); the Africa-Adria-related ALCAPA (i.e., Alpine-Carpathian-Pannonian) Unit and the Europe-related Tisza-Dacia Unit (Figure 1a). These units were juxtaposed along the ENE-WSW striking Mid-Hungarian Shear Zone (MHSZ) during the Early to earliest Middle Miocene times (Balla, 1988; Csontos & Nagymarosy, 1998; Fodor et al., 1998; Kázmér & Kovács, 1985; Tari, 1994). This displacement was part of the broader Alpine-Carpathian deformation process generally called lateral extrusion (Ratschbacher et al., 1989). Within or just along this shear zone several smaller-scale tectonic units are present, all of which show close relation to the pre-Miocene stratigraphy and structures of the Southern Alps and northwestern Dinarides (Haas & Kovács, 2001; Kovács, 1982).

The nappe system of the Bükk Unit in the northern Pannonian Basin is one of these far-traveled units originating from the junction area of the Southern Alps or northwestern Dinarides, ca. 500–600 km to the SW in present day coordinates (Figure 1a; Csontos, 2000; Kovács, 1984; Schmid et al., 2008). The structural boundaries of the Bükk Nappe System (BNS) are mostly covered by Cenozoic sediments, thus the characterization of its boundary is difficult. However, deep boreholes indicate that it is bordered by the MHSZ from the south and it has a contact with the Transdanubian Range Unit, and through that with the ALCAPA Unit toward the west. Schmid et al. (2008) presumed that this western boundary coincided with the so-called Darnó Deformation Zone running in NNE-SSW direction, but borehole core analysis has proved that the BNS continues west of the Darnó Zone as well (Recsk Unit in Figure 1; Fodor et al., 2017). The only partly exposed boundary of the BNS is in the north, where its Paleozoic and Mesozoic formations are thrust over the Paleozoic and Upper Cretaceous formations of the Uppony Unit along the Nekézseny Thrust (NT) (Figure 1b; Less et al., 2002; Pelikán et al., 2005; Schréter, 1945). The Uppony Unit (UpU) is the southernmost exposure of the Inner Western Carpathians (as part of the ALCAPA Unit) and correlates with the Upper Austroalpine Units in the Alps (Kovács et al., 2011; Plašienka, 2018; Schmid et al., 2008, 2020; Vozár et al., 2010).

The age of these tectonic contacts has primary importance concerning the tectonic evolution of the area: the blocks derived from the Southern Alps or the Dinarides were either amalgamated to the ALCAPA Unit before the major Miocene shearing along the MHSZ, thus can be interpreted as integral parts of the ALCAPA block already in the late Paleogene (Balla, 1984; Csontos & Vörös, 2004), or they form separate tectonic units which were

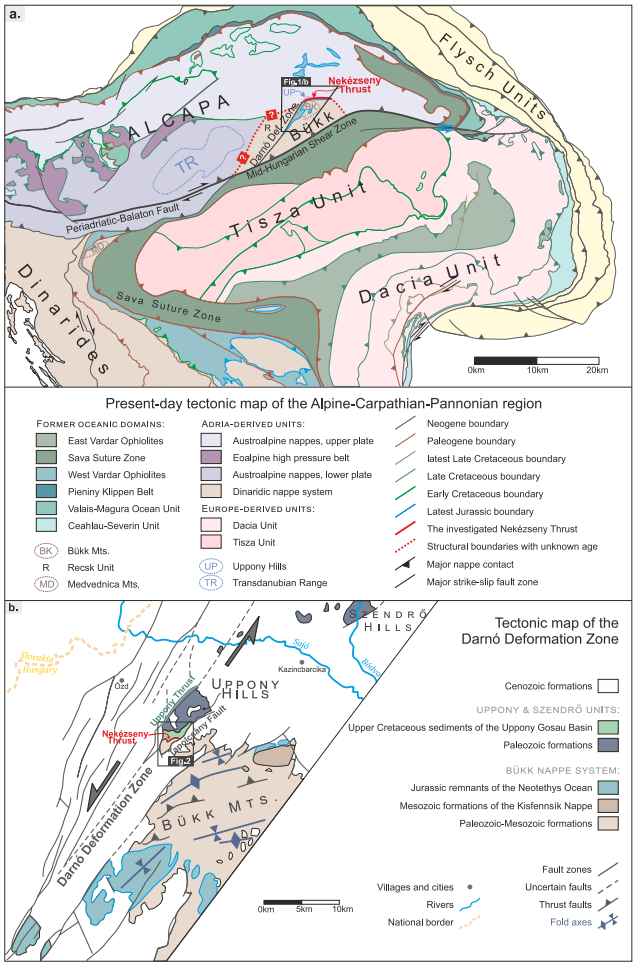

Figure 1. Tectonic position of the study area. (a) Large-scale position of the Bükk Nappe System and Uppony Unit within the Alpine-Carpathian-Dinaric area (modified after Schmid et al. (2008, 2020)). According to Schmid et al. (2008), the Bükk Nappe System is built up by a displaced part of the Inner Dinaric Nappe System, while the Uppony Unit is part of the Austroalpine ALCAPA Unit. (b) Tectonic map of the study area in the northern part of the Darnó Deformation Zone (modified after Fodor et al. (2005)). The Nekézseny Thrust separates the Bükk Nappe System in the south from the ALCAPA-related Paleozoic and Upper Cretaceous formations of the Uppony Unit in the north.

sheared off from their original place on the Adriatic plate during the late Oligocene to Miocene activity of the shear zone (Haas et al., 2010; Schmid et al., 2008; Ustaszewski et al., 2008). In the first case, the units should have pre-Miocene contacts toward the other sub-units of ALCAPA, while the second case denotes that their boundaries are Miocene in age and the Dinarides-derived units moved to their present-day position during the activity of the Mid-Hungarian Shear Zone.

2.1. Tectonic Context of the Nekézseny Thrust

The NE-SW striking **Nekézseny Thrust (NT)** forms the southeastern structural boundary of the UpU, and juxtaposes its Paleozoic and Upper Cretaceous ("Senonian") formations with the Permo-Mesozoic formations of the BNS (Figures 1b and 2, Schréter, 1953). Due to the lack of any Paleogene sediments in the close vicinity of the NT, the age of thrusting has only been estimated based on regional observations. For instance, the **Uppony Thrust (UT)** running along the northwestern boundary of the UpU runs almost parallel to the NT and places Upper Paleozoic formations over sheared Triassic limestone blocks, Upper Oligocene and Lower Miocene formations (Figures 1b and 2), suggesting Oligocene to Early Miocene age for the thrusting. Fodor et al. (1992, 2005) considered both thrusts to be part of the **Darnó Deformation Zone** running along the western part of the BNS and UpU, which was a significant transpressional fault zone with reverse or left-lateral character during the Oligocene and Early Miocene (Fodor et al., 1992, 2005; Pantó, 1954; Schréter, 1945; Telegdi Roth, 1951; Zelenka et al., 1983). However, some authors suggested that the precursory of the Darnó Zone might have originally been inherited from Cretaceous times (Csontos, 1999; Fodor et al., 2023).

Regarding the Cretaceous deformation of the BNS and UpU, the tectonic transport direction was just the opposite in the two adjacent units (top-to-S or -SE in the BNS and top-to-N or -NW in the UpU, Csontos, 1999; Koroknai, 2004; Pelikán et al., 2005; Schréter, 1945). This structural difference and other paleogeographic considerations led Schmid et al. (2008) to assign them to completely different paleogeographic units: the BNS to the Inner Dinaridic Nappe System and the UpU to the southernmost Inner Western Carpathians as part of the ALCAPA Unit. Note that this concept of the ALCAPA Unit refers to a Cretaceous nappe system with specific Mesozoic paleographic meaning (see details in Schmid et al. (2008)).

Furthermore, in close vicinity of the NT, Fodor et al. (1992) and Less et al. (2002) mapped another NE-SW striking fault, the **Tapolcsány Fault** (**TF**, Figures 1b and 2). This fault presently shows normal displacement which post-dates the deposition of the Lower Miocene formations in its hanging wall and partly displaces the NT, further complicating its geometry. Considering this, the NT has probably suffered multiple reactivations but its initial age and early deformation history have remained unconstrained.

2.2. Tectonic Evolution of the Bükk Nappe System and Uppony Units

The BNS and the UpU were part of the Adriatic plate during the Mesozoic, and their tectonic evolution was linked to the evolution of two bordering oceanic domains, the southeastern Neotethys Ocean and the northwestern Alpine Tethys Ocean. While only Paleozoic formations and Late Cretaceous Gosau-type sediments are present in the UpU, the BNS is built up by Paleozoic and Mesozoic formations ranging from the Carboniferous to the late Middle Jurassic. During the Permo-Triassic rifting and subsequent late Middle Triassic to Middle Jurassic spreading of the Neotethys Ocean, both units were located in the western part of the Neotethys embayment (Haas et al., 1995; Schmid et al., 2008). In the area of the future BNS, rapid subsidence during the late Anisian to early

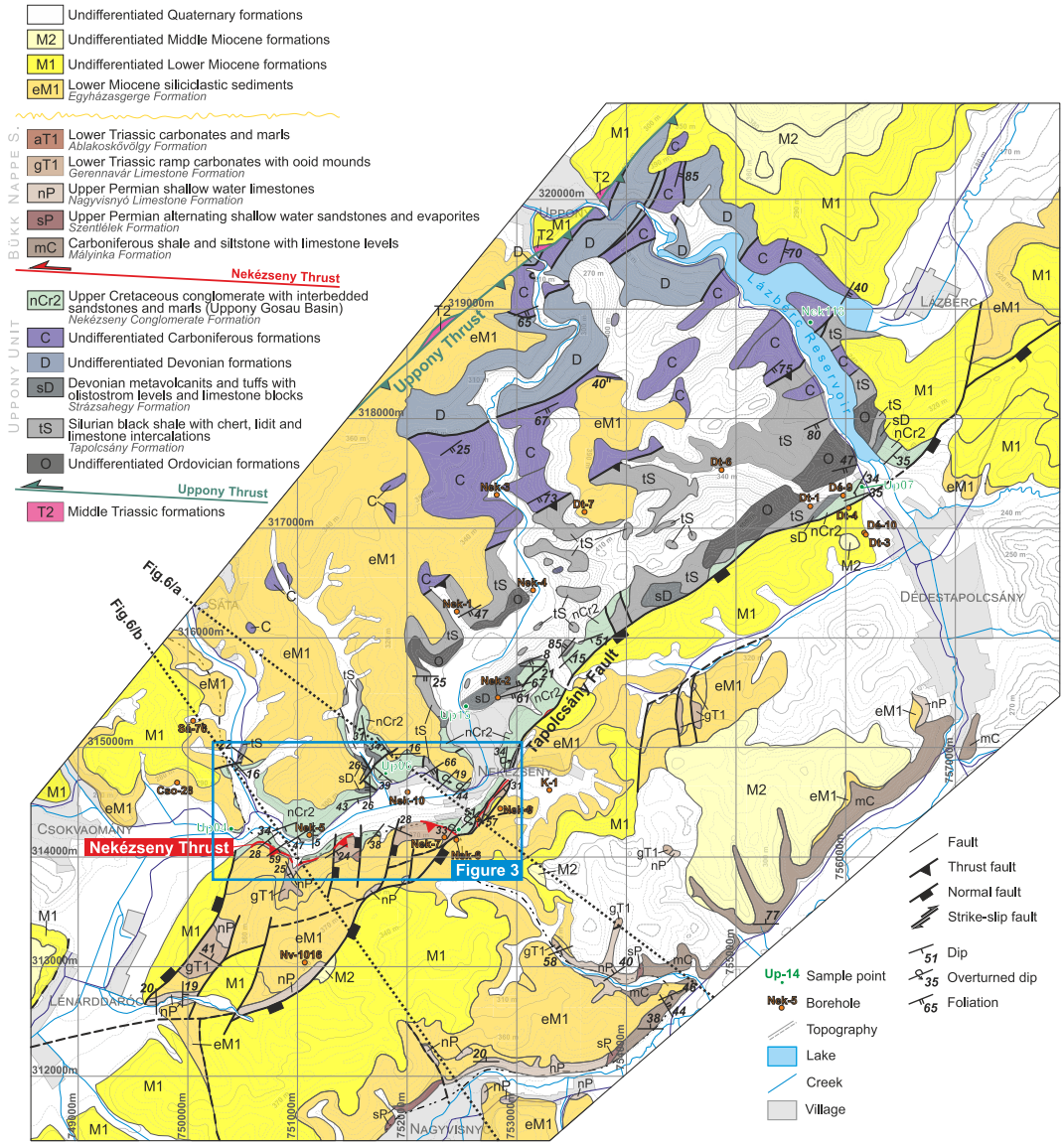

Figure 2. Geological map of the boundary area between the Bükk Nappe System and Uppony Unit (modified after Less et al. (2002)). Coordinates are set in the National Hungarian Grid (EOV) system.

Ladinian and syn-rift andesitic volcanism mark the onset of the continental break-up (Haas et al., 2011; Szoldán, 1990; Velledits, 2006). As a result, the previous ramp environment was fragmented, and carbonate platforms separated by intraplatform basins developed (Velledits, 2006). The general subsidence continued and hemi- to eupelagic siliciclastic sedimentation with frequent mass movements became widespread during the Middle Jurassic (Haas et al., 2011, 2013).

During the latest Early Jurassic, the extensional tectonic regime changed to contraction due to intra-oceanic subduction initiation in the Neotethys Ocean. This intra-oceanic subduction turned into obduction in the Late Jurassic, during which Adria was in lower plate and the oceanic lithosphere of the Neotethys in upper plate position (Handy et al., 2015; Maffione & van Hinsbergen, 2018; Schmid et al., 2008). While obducted ophiolites are widespread in the Dinarides (Dimitrijević & Dimitrijević, 1973; Pamić et al., 2002), the sensu stricto ophiolite nappe is absent from the BNS, although a slice of the sub-ophiolitic mélange is preserved (Darnó Mélange Complex, Kovács et al., 2008, 2011). Additional indications for its former presence are the redeposited serpentinite and basic (meta)magmatitic rock pebbles found in Lower Miocene conglomerates (Sztanó & Józsa, 1996). The Late Jurassic to Early Cretaceous shortening and nappe stacking resulted in the development of

the BNS (Csontos, 1999, 2000; Haas & Kovács, 2001), which was accompanied by large-scale folding and thrusting in both the BNS and UpU. This main folding event re-folded the original $S_{0\text{-}1}$ layer-parallel foliation and resulted in the S_2 (axial plane) foliation which dominates the structure of both units (Csontos, 1999; Koroknai, 2004). The Neotethys remained open up to the collisional phase, and the last remnants of this ocean and related tectonically truncated units are found within the Sava Zone (Channell et al., 1979; Schmid et al., 2008; Stojadinovic et al., 2022). The onset of collision of Adria and Tisza-Dacia Unit (Europe) was dated to the Maastrichtian (70.6–65.5 Ma, Ustaszewski et al., 2009, 2010) and continued to cause contraction during Paleocene to earliest Miocene times. In the BNS and UpU, younger folds and thrusts overprinted the first-order Cretaceous structures (Csontos, 1999; Fialowski, 2018; Scherman, 2018), but their timing and eventual correlation with other tectonic events in the Alps, Carpathians, or the Sava Zone remained uncertain due to lack of narrow age constraints. Apatite fission-track data from the lowermost nappe of the BNS seem to suggest slow cooling between 53 Ma (upper nappes) and 43 Ma (Árkai et al., 1995), but its relation to deformation or erosion is unclear.

Afterward, the continuous northward movement of Adria led to the Oligocene to Early Miocene east-directed lateral extrusion of the complete ALCAPA Unit from the Austroalpine domain toward the present-day Pannonian embayment (Balla, 1988; Csontos & Nagymarosy, 1998; Fodor et al., 1998; Kázmér & Kovács, 1985; Ratschbacher et al., 1989). The southern boundary of the extruding ALCAPA was the Mid-Hungarian Shear Zone, which lies in the continuation of the Periadriatic Fault of the Alps, and it is inferred to have accommodated several hundreds of kilometer displacement in the Pannonian Basin (Tari, 1994).

Following the extrusion, subduction roll-back in the Eastern Carpathians resulted in back-arc extension and the formation of the Pannonian Basin between 20 and 9 Ma (Balázs et al., 2016; Csontos, 1995; Horváth et al., 2006; Tari et al., 2023). The extension was accompanied by the counterclockwise rotation of the ALCAPA (Márton & Márton, 1996), and led to the development of several extensional/transtensional phases (Fodor et al., 1999; Petrik et al., 2016).

2.3. Stratigraphy of the Bükk–Uppony Boundary Zone

The UpU is dominantly built up by Paleozoic formations (Figure 2), which were not affected by Variscan metamorphism, but underwent low-grade Eoalpine metamorphism. Due to this overprint and the paucity of fossils, accurate stratigraphic constraints are sporadic, but based on Alpine analogies the age of these formations ranges from the Late Ordovician to Late Carboniferous (Pelikán et al., 2005). In the southern UpU, the oldest mapped formations are dark gray or black shales, interbedded with thin chert, lydite or limestone layers (Tapolcsány Formation). This shale formation was correlated to the characteristic graphite and lydite-bearing Silurian black shales of the European area (Kovács et al., 1983; Pelikán et al., 2005). The black shale is followed by a mixed formation of basic metavolcanites, light gray crinoidal and metasomatized limestones, interbedded by coarse olistostrome levels (Strázsahegy Formation, Pelikán et al., 2005).

In the UpU prove that the Paleozoic sedimentation continued until the Late Carboniferous (Pelikán et al., 2005), approximately when the deposition of the Paleozoic succession of the BNS started. Here the Variscan flysch basin was completely filled by Lower Permian, and a gently dipping ramp formed first with shallow water sandstones and evaporites (Mályinka and Szentlélek Formations), then with thin-bedded dark limestones with black marl intercalations and rich shallow water flora (Nagyvisnyó Limestone, Figure 2; Less et al., 2002; Pelikán et al., 2005). The Permian–Triassic boundary is marked by a sharp sedimentary contact and disappearance of this rich Permian flora (Hips & Haas, 2006). The facies of the overlying carbonates suggests that ooid mounds became dominant in the inner ramp environment during the earliest Early Triassic (Gerennavár Limestone, Hips & Pelikán, 2002), followed by the gradual increase of terrigenous input, as indicated by the alternation of carbonates and fine-grained siliciclastics during the second half of the Early Triassic (Ablakoskővölgy Formation, Pelikán et al., 2005). In the Ladinian, extensive shallow water carbonate sedimentation initiated and had continued, until the carbonate platforms were disrupted and drowned due to the deepening of the Neotethys Ocean (Velledits, 1999, 2004).

After a major hiatus, the metamorphosed Paleozoic formations of the UpU are covered by non-metamorphic conglomerates of the Uppony Gosau Basin, which deposited from coarse-grained gravity flows initiating in alluvial fans (Nekézseny Conglomerate, Figures 1 and 2; Balogh, 1964; Brezsnyánszky & Haas, 1984; Clifton et al., 1985; Pelikán et al., 2005; Schréter, 1945). Rudists and foraminifera fossils suggested Santonian to

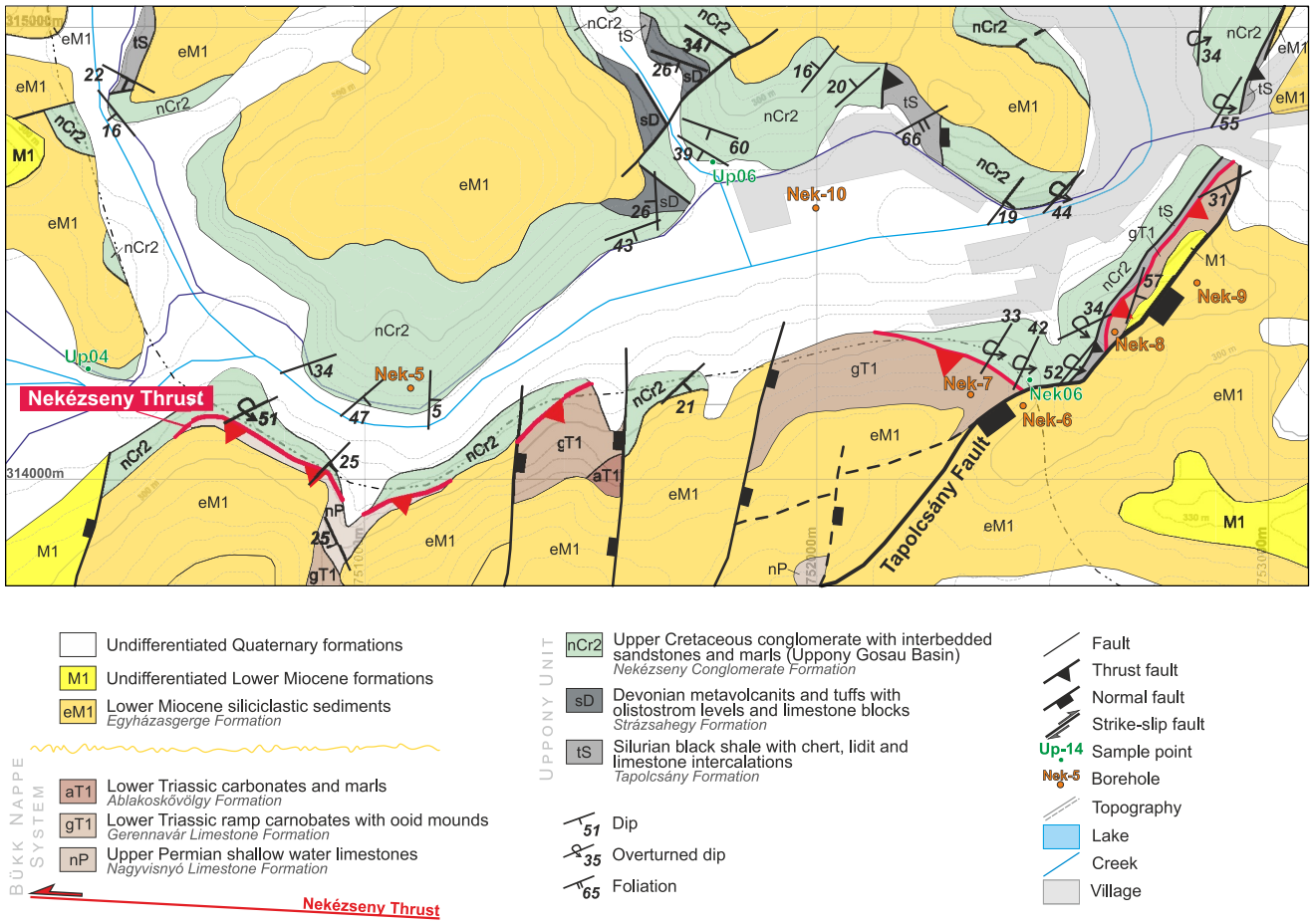

Figure 3. Enlarged geological map of the most exposed parts of the Nekézseny Thrust and the large overturned limb of the recumbent fold located directly below the structural contact. See map legend in Figure 2.

Campanian age for this conglomerate (Schréter, 1945), while the palynological studies rather argued for Campanian age (Sieglné Farkas, 1984). Pebble composition analysis showed that the Gosau basin received sediments from almost every nearby units (UpU, Szendrő, Aggtelek, and Rudabánya Hills), except from the present-day neighboring Bükk Mts (Brezsnyánszky & Haas, 1984; Clifton et al., 1985).

The pre-Cenozoic formations of the BNS and UpU are mostly covered by Miocene formations, with the complete lack of Paleogene in the study area (Figure 2). The Cenozoic formations are mainly Lower Miocene sandstones, siltstones and claystones (Egyházasgerge Formation), covered by Early to Middle Miocene clastics and volcanoclastics (Less et al., 2002; Lukács et al., 2022; Pelikán et al., 2005).

3. Methods

3.1. Structural Data and Borehole Core Analysis

Detailed geological mapping and mesoscopic structural observations were carried out in the transitional zone between the UpU and BNS in NE Hungary, where their structural contact is exposed on the surface (NT, Figures 2 and 3). Further sedimentological observations contributed to recognizing overturned sections of the Upper Cretaceous conglomerate in the field. The pre-Campanian deformation and metamorphosis of the Paleozoic and Triassic formations are not discussed here (see Koroknai, 2004; Pelikán et al., 2005). Our observations were compared to the geological maps of Less et al. (2002), and we constructed an updated geological map for the Bükk-Uppony transitional area and two cross-sections.

The field observations were followed by stereographic fault-slip analysis and fold axis estimations. By using the analytical method of Angelier (1984), the evaluation of the structural data was carried out separately at first for each locality, then the individual results were compared and combined. The data were either separated manually or where at least four fault striae reflected the same stress field, automatic data separation was also possible. Tilt-tests were carried out when the geometrical characteristics of the faults and folds indicated pre-tilt deformation (e.g., the symmetry plane of the conjugate faults was perpendicular to the bedding, thickness variations and onlap surfaces were observed within the deformed layers). Relative chronological order of the separated phases was determined based on the observed deformation geometries (pre-tilt or post-tilt faults), cross-cutting fractures, and superimposed striae on reactivated surfaces.

Five boreholes (Nek-6, -7, -7a, -8, -8a) were selected for revision and microtectonic analysis, all of which were drilled in close vicinity of the NT (Figure 2). Thin sections were prepared and inspected via an optical microscope.

3.2. Apatite Fission-Track Thermochronology

Samples for apatite fission-track (AFT) analysis were prepared from the 63–125 μm fraction from four Upper Cretaceous sandstone samples and one Devonian metavolcanic sample (Strázsahegy Fm., see sample localities in Figure 2). The apatite grains were concentrated by conventional heavy mineral separation techniques, including crushing and sieving as well as magnetic- and heavy-liquid separation. Handpicked grains were mounted in epoxy resin, then ground and polished in two (P1200 and P2500) and three (9, 3, and 1 μm) steps, respectively.

Spontaneous fission tracks were revealed by etching with 5.5 M HNO_3 at 20°C for 20 s. Samples were analyzed by the external detector method (EDM, Gleadow, 1981) using very low uranium muscovite mica detectors, and irradiated at the Oregon State University Triga Reactor, Corvallis, USA. Neutron fluence was monitored using CN5 uranium-doped glass. After irradiation, induced tracks in the mica external detectors were revealed by etching with 40% HF for 20 min. Fission tracks were counted at the Institute for Nuclear Research of Hungary by an Olympus BX53 microscope equipped with a microscope-computer-controlled stage system with 1000x magnification (Dumitru, 1993). Central ages (Galbraith & Laslett, 1993) were calculated by the TRACKKEY software (version 4.2.g; Dunkl, 2002) based on the approach of Hurford and Green (1983), whereas radial plots were created via DensityPlotter (Vermeesch, 2012). A personal zeta-calibration factor of 286.7 ± 4.6 was obtained by calibration against the Durango apatite and Fish Canyon Tuff apatite age standards according to Hurford (1990).

3.3. K/Ar Geochronology

Clay-rich fault gouge samples were collected from the Nek-7, Nek-7a, and Nek-8a boreholes for K/Ar dating (see sample locations in Figure 7). The samples were mildly crushed with a laboratory rotor mill, and the fine powder was suspended in water glass columns. Coagulation of the eventually present charged particles was prevented by washing the samples by de-ionized water in ultrasonic bath and by adding sodium-polyphosphate to the samples. Following Stoke's law, the <5 μm and the <2 μm fractions were extracted at 23°C ambient temperature after 65 and 406 min from the upper 10 cm segment of the water column. The removed suspension was then dried at 50°C in order to prevent Ar loss from the samples. Separation of the >0.2, >0.5, and 1 μm fractions was performed in a large volume centrifuge using the centrifuge parameter calculation of Tributh and Lagaly (1986).

The mineral composition of the separated samples was controlled by X-ray powder diffraction (XRPD) method at the Mineralogical Department of the Eötvös Loránd University, Budapest. The analyses were performed on a Philips PW-1730 diffractometer equipped with a graphite monochromator using Cu-Kα radiation at 45 kV and 35 mA with 1° divergence slit and 1° receiving slit. Scanning rate was 0,05°2Θ per minute from 3° to 70°. The determination of the semi-quantitative mineral composition is based on XRD.

The separated illite fractions were analyzed by K-Ar method, using the un-spiked peak comparison method in the K-Ar laboratory of the Institute for Nuclear Research, Debrecen. Potassium content was measured on 50 mg sample aliquots, after dissolution by HF and HNO_3, with a Sherwood-400-type flame spectra-photometer with accuracy better than ±1.0%. Separated mineral sample splits were then subjected to heating at 100°C for 24 hr under high- vacuum, to remove atmospheric Ar contamination that was adsorbed on the surface of the mineral particles during sample preparation. Ar was extracted from the minerals by fusing the samples via high-frequency induction heating at 1300°C. The released gas was cleaned in two steps in a low-blank vacuum system by St-707

10.1029/2023TC008189

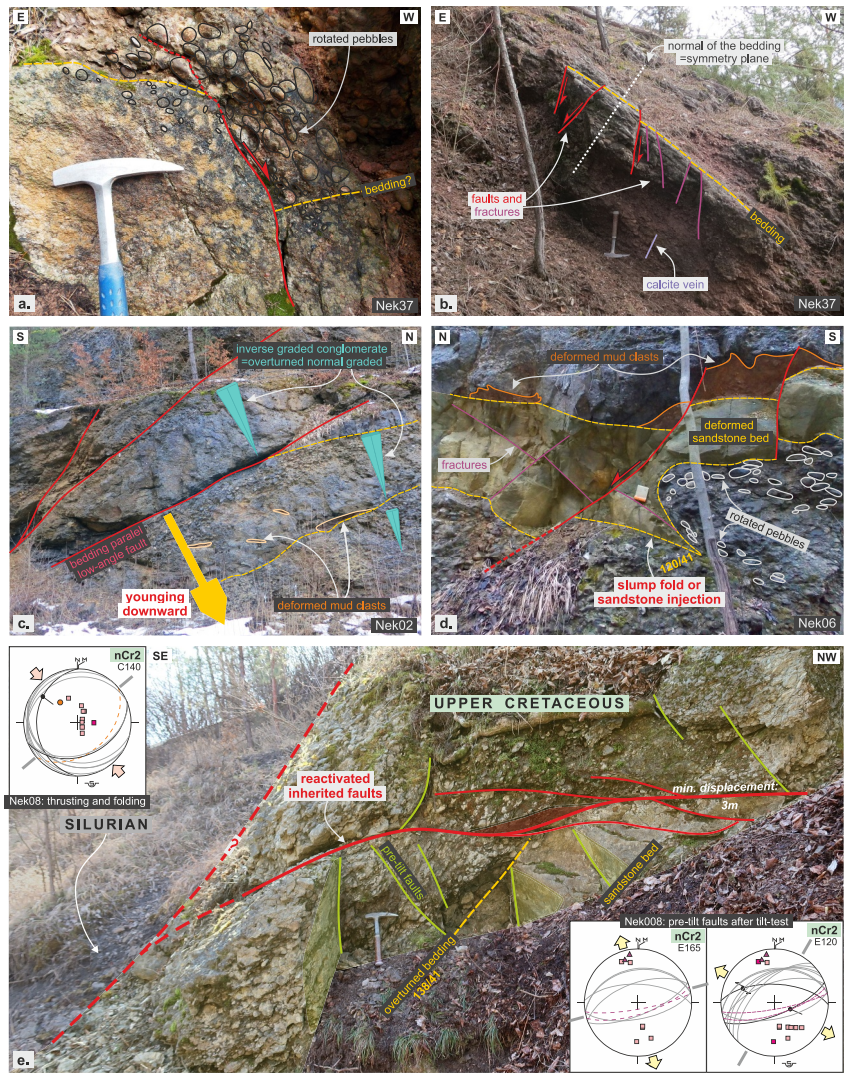

Figure 4. Interpreted field photos and stereoplots from the Upper Cretaceous conglomerate. (a) Syn-sedimentary/syn-diagenetic normal fault, with "plastically" rotated pebbles along the sealed fault plane. (b) Conjugate pre-tilt normal faults and fractures. The discrete fault planes suggest post-cementation deformation, however, symmetry axes of the conjugate fault pairs are perpendicular to the tilted bedding planes, which suggest normal faulting prior to tilting. (c) Presently upward coarsening of the Upper Cretaceous conglomerate, which is interpreted as overturned normal grading. (d) Downward directed sandstone injection dyke, indicating overturning position of the Upper Cretaceous formation. (e) Field photo and stereoplots of the immediate contact zone of the Silurian and Upper Cretaceous formations. The contraction reactivated the pre-tilt fractures. Two groups of these faults were separated: the E-W striking normal faults were probably overprinted by the second group of NE-SW striking faults. See stereoplot legend in Figure 5.

and Ti-getters. The isotopic composition of the Ar was measured using a Nier-type Argus VI© mass multi-collector spectrometer and corrected for the atmospheric $^{40}Ar/^{36}Ar$ ratios measured day-to-day. The accuracy and reproducibility of isotope ratio measurements were periodically controlled with the HDB-1 (Hess & Lippolt, 1994) and GL-O (Odin, 1982) international standards. Decay constants recommended by Steiger and Jäger (1977) were used for age calculation, with an overall error of ±1%. Error of the analyses was calculated using the equation of Quidelleur et al. (2001).

3.4. Apatite (U-Th)/He Thermochronology

Three samples were collected (two from Upper Cretaceous sandstones and one from Carboniferous sandstones, see localities in Figure 2) for apatite separation and (U-Th)/He thermochronology (AHe). Two to six single-

crystal aliquots were selected from each sample, based on the selection criteria that they should be inclusion- and fissure-free, intact, mostly euhedral grains with more than 65 μm width. The crystals were wrapped in 1 × 1 mm platinum capsules, then heated in the full-metal extraction line by an infra-red laser in vacuum. Purification of the extracted gas was done by using a SAES Ti-Zr getter kept at 450°C. This was followed by the expansion of the chemically inert noble gases and a minor amount of the other rest gases into a Hiden triple-filter quadrupol mass spectrometer. Sequential reheating and He-measurements were carried out to check all the crystals for degassing of He. Following the degassing, the samples were retrieved from the gas extraction line, spiked with calibrated ^{230}Th and ^{233}U solutions. The apatite crystals were dissolved in a 2% HNO_3 + 0.05% HF acid mixture in Savillex Teflon vials, then the spiked solutions were analyzed by a Thermo iCAP Q ICP-MS coupled to an autosampler. The concentration of actinides was determined by isotope dilution and the Ca, Sm and the REEs were determined by external calibration. Finally, the ejection correction factors were calculated for every single crystals by using the modified algorithms of Farley et al. (1996). The AHe ages were calculated by the Taylor Expansion Method after Des Patterson.

4. Structural Observations and Kinematic Analysis

4.1. D_1: Pre-Tilt (Partly Syn-Diagenetic) Extension

A series of outcrop-scale conjugate normal fault pairs were observed in the Upper Cretaceous conglomerate; some of them have discrete fault planes, while others have sealed (cemented) fault planes (Figure 4a). In the latter case, thickening of the distorted layers toward the normal faults is common, and the faults are often covered by the subsequent undeformed layers. The symmetry axes of the conjugate normal faults are perpendicular to the tilted bedding planes, suggesting pre-tilt geometry (Figure 4b). This means that these normal faults formed prior to the tilting and folding of the layers, that is, when the bedding was still horizontal; as opposed to post-tilt structures, which form in already tilted layers and overprint the folding event. Pebble alignment along the normal faults was also observed, meaning that the otherwise un-oriented pebbles rotated until their longest axis became parallel to the fault planes (Figure 4a). To explain the pebble rotation, the fine-grained matrix of the conglomerate must have still deformed "plastically" at the time of the normal faulting. This implies that the Upper Cretaceous conglomerate was first deformed in a soft- or in semi-consolidated state.

The above-mentioned syn-sedimentary to syn-diagenetic deformation structures may have formed solely in response to atectonic slope-related sedimentary processes. However, pre-tilt normal faults with discrete fault planes prove that the extension continued even after the consolidation (cementation). This suggests tectonic origin at least for a part of the observed early normal faults (D_1 phase). Regarding their original orientation, the strikes of the pre-tilt normal faults show strong scattering between NW-SE and NE-SW, but a large number of them strike in NE-SW direction (Figure 5).

4.2. D_2: Top-To-NW Thrusting and Folding

Around the village of Nekézseny, the Permo-Triassic formations of the BNS are exposed above the metamorphic Paleozoic and non-metamorphic Upper Cretaceous formations of the UpU (Figure 3). Their contact zone (NT) is a SE-ward dipping low-angle fault zone east of Nekézseny, while it flattens to sub-horizontal geometry southward (Figure 6). Below the contact zone, the Upper Cretaceous conglomerate is folded into gentle to open folds with NE-SW trending axes and top-to-NW tectonic transport direction. However, at the low-angle segment, the shallow to moderately (20–40°) southward dipping conglomerate is overturned and forms a large map-scale recumbent fold. The overturned position of the moderately (25–50°) dipping beds is inferred from sedimentary observations (already described by Brezsnyánszky and Haas (1984) and Clifton et al. (1985)), such as apparent inverse grading of the conglomerate (Figure 4c) and downward directed sandstone injection dykes (Figure 4d). A thin sheet of Silurian is thrust over the overturned limb of the recumbent fold (Figure 3, near the Nek-8 borehole). In the Cretaceous rocks, there is no gradual transition between the overturned and normal limbs, only a sharp change of polarity can be detected, indicating a fault contact between them. The contractional structures observed in the Upper Cretaceous rocks are truncated and discordantly covered by the upper Lower Miocene formations (Figures 2 and 3).

Beside the NT itself, further map-scale thrust faults are postulated that deformed the Upper Cretaceous beds. They were not recognized directly on the field, however, geological mapping proved that several of the Paleozoic—Upper Cretaceous contacts are not sedimentary boundaries as previously believed, but low-angle tectonic

10.1029/2023TC008189

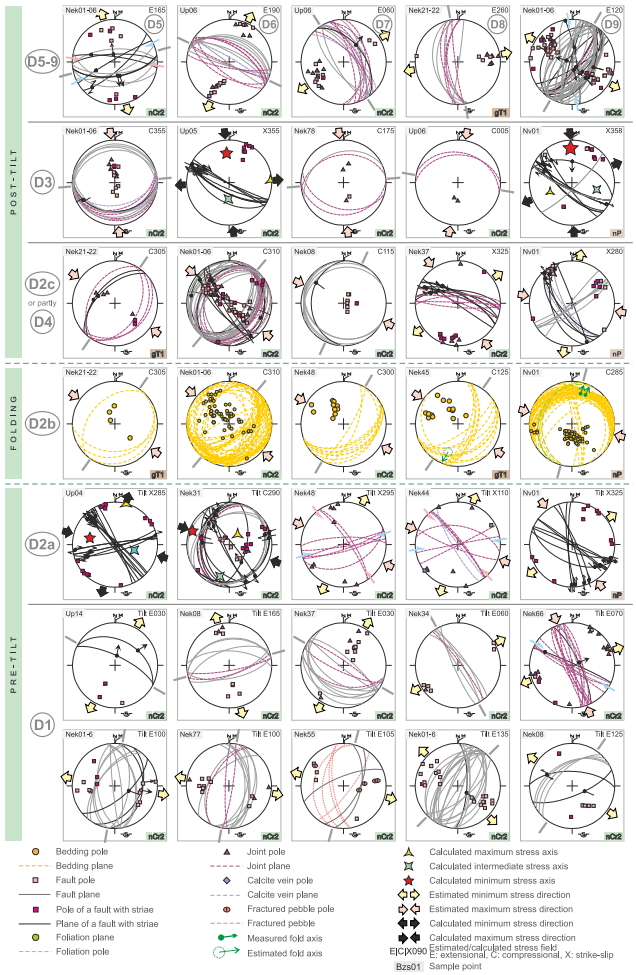

Figure 5. Table of selected stereoplots from the interpreted deformation phases. The pre-tilt D_1 phase is related to development of the Uppony Gosau Basin. Emplacement of the BNS over the UpU and coeval folding of the Upper Cretaceous conglomerate happened in the D_2 phase. C, X, E signal compressional, strike-slip and extensional stress states, respectively; the numbers refer to the direction of σ_1 (C, X) and σ_3 (E). Where the word "Tilt" is used before the estimated/calculated stress field direction, all the data presented on the stereoplots are back-tilted with the local average bedding dip data, so that their original pre-tilt geometry is restored. See the complete list of data localities in the data set of Oravecz (2023).

contacts with pre-Miocene age. This is evidenced by the Cretaceous formations apparently dipping under the Paleozoic ones, while the sealing base-Miocene unconformity remains continuous and doesn't show any displacement (Figures 2 and 3). Similar NE-SW striking thrust faults are also present in the hanging wall block of the NT, as inferred from the mapped repetition of the Permo-Triassic formations north of Nagyvisnyó (Figure 6; Juhász et al., 2021). In close vicinity of the NT, outcrop-scale thrusts cross-cut the overturned Upper Cretaceous conglomerate (Figure 4d). These thrust faults are always low or very low-angle shear zones with respect to the local dip, often flatten into the bedding planes, and have NE-SW strike. By restoring the original horizontal position of the Upper Cretaceous, the tectonic transport direction of these thrusts is top-to-NW. In some cases, the contraction evidently favored the reactivation of tilted normal faults formed during the D_1 phase (Figure 4e).

Considering these observations, the NT is a NW-vergent structural contact that formed during NW-SE contraction. The related D_2 phase may be subdivided into a D_{2a} pre-tilt, D_{2b} syn-tilt and D_{2c} post-tilt events (Figure 5). While the deformation directly at the low-angle segment of the NT seems to be purely contractional, further away E-W and WNW-ESE striking dextral and NW-SE and NNW-SSE striking sinistral strike-slip faults with reverse character were observed, that rather suggest transpressional deformation. The overall inferred shortening directions scatter between WNW-ESE and NW-SE.

4.3. D_3: N-S Shortening

A post-tilt N-S or NNW-SSE directed shortening phase is inferred from the fault-slip analysis (Figure 5). The related structures are outcrop-scale E-W striking low-angle thrust faults and NW-SE striking dextral strike-slip faults, that frequently overprint the structures associated with the D_2 phase. Map-scale structures were not recognized.

4.4. D_4: NW-SE Shortening

A few weak striae superpositions suggest that there was another NW-SE shortening (D_4) phase after the D_3 phase. This is also supported by regional consideration, that is, a late-stage thrusting event is documented north of the study area, along the UT (Figure 2; Fodor et al., 2005; Kovács et al., 2020), that deformed the Paleogene and Lower Miocene formations. As the D_{2c} and D_4 phases have similar stress axes, the age of the post-tilt structures reflecting NW-SE σ_1 is not well constrained, and those elements could also be classified into either or both deformation phases. The stereograms are represented together in Figure 5.

4.5. D_5-D_9: Extensional Phases

Discrete normal faults, joints and deformation bands with presently high-angle geometry, sometimes with striations and calcite vein precipitation were often observed in the area, even within Miocene sedimentary rocks. The normal faults displace every previously described structural element. Based on their orientation and previous fault analysis results from nearby study areas (e.g., Beke et al., 2019; Fodor et al., 2005; Petrik et al., 2016), the post-tilt extensional structures were separated into five extensional phases (D_5-D_9, Figure 5). They are, successively, Early Miocene ~ N-S, NNE-SSW, and NE-SW extension, Middle Miocene E-W extension, and Middle to Late Miocene NW-SE extension (Beke et al., 2019). The most noteworthy young normal fault in the area is the NE-SW striking, SE-ward dipping TF that displaces Lower and Middle Miocene formations (the fault was dissected by the

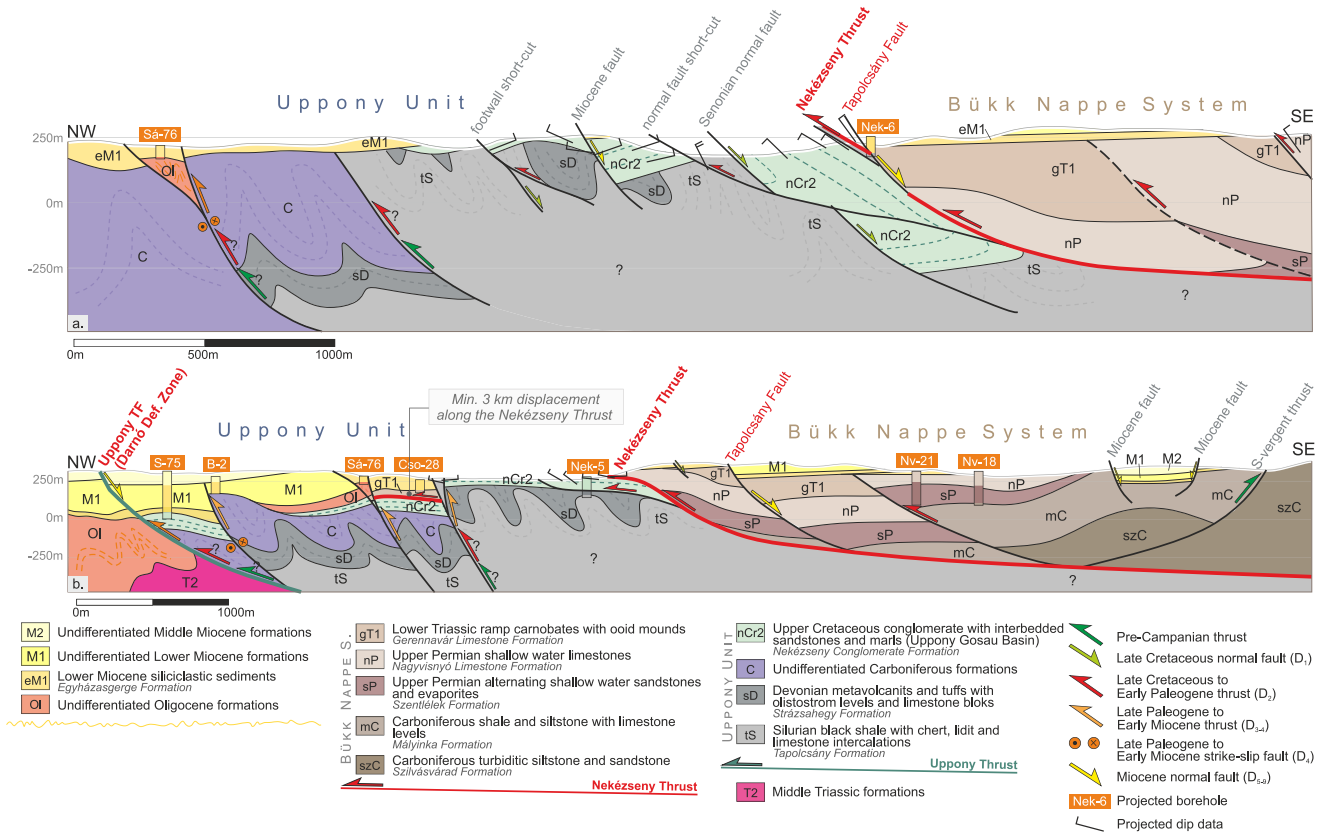

Figure 6. New cross-sections through the study area. See the section trace lines in Figure 2. (a) Section through the large overturned Upper Cretaceous sliver and the exposed ramp segment of the Nekézseny Thrust. (b) Section through the exposed flat segment of the Nekézseny Thrust and the westernmost known occurrence of the Mesozoic formations of the BNS in the *Cso-28* borehole. The depth of the detachment is only conceptual and not constrained by sub-surface data.

Nek-6 borehole, see later). North of Nekézseny, the TF runs approximately along the NT, however, it deviates from the NT and cuts into the Permo-Mesozoic formations of the BNS southward (Figure 2).

5. Observed Superpositions in Boreholes and Microtectonics

5.1. Silurian on Upper Cretaceous: Nek-6, -8, -8a Boreholes

The Nek-6 borehole starts in semi-consolidated fine-grained gray sandstone with claystone and siltstone intercalations (Figure 7a). The sandstone contains micas and mollusk fragments in large quantities, as well as deformation bands, which are all characteristic features of the late Early to earliest Middle Miocene formations (Pelikán et al., 2005). The adjacent Nek-8 and -8a boreholes start with (Figures 7d and 7e) and the Nek-6 continues in a weathered and macroscopically structureless dark gray siltstone, although locally some remanent foliation could still be observed macroscopically. Thin sections revealed that the massive-looking siltstone is actually a cataclasite, where relatively well-foliated clasts are surrounded by a fine-grained matrix (Figure 8a). These sections are interpreted as deformed parts of the Silurian shale.

The Silurian is underlain by the diverse, grain-supported Upper Cretaceous conglomerate in all three boreholes (Figures 7a, 7d, and 7e). Its upper sections are strongly deformed: fractured clast fragments are embedded in fine-grained matrix, some of them are re-worked cataclasites themselves, suggesting multiphase renewal of the deformation (Figure 8b). The re-worked cataclasite clasts are often bounded by pressure solution marks (stylolites). While the cataclastic pattern gradually disappears downward and the undeformed sedimentary pattern with rounded pebbles gets restored, the Nek-8a borehole contains another cataclastic zone at around 13 m depth (Figure 7e).

10.1029/2023TC008189

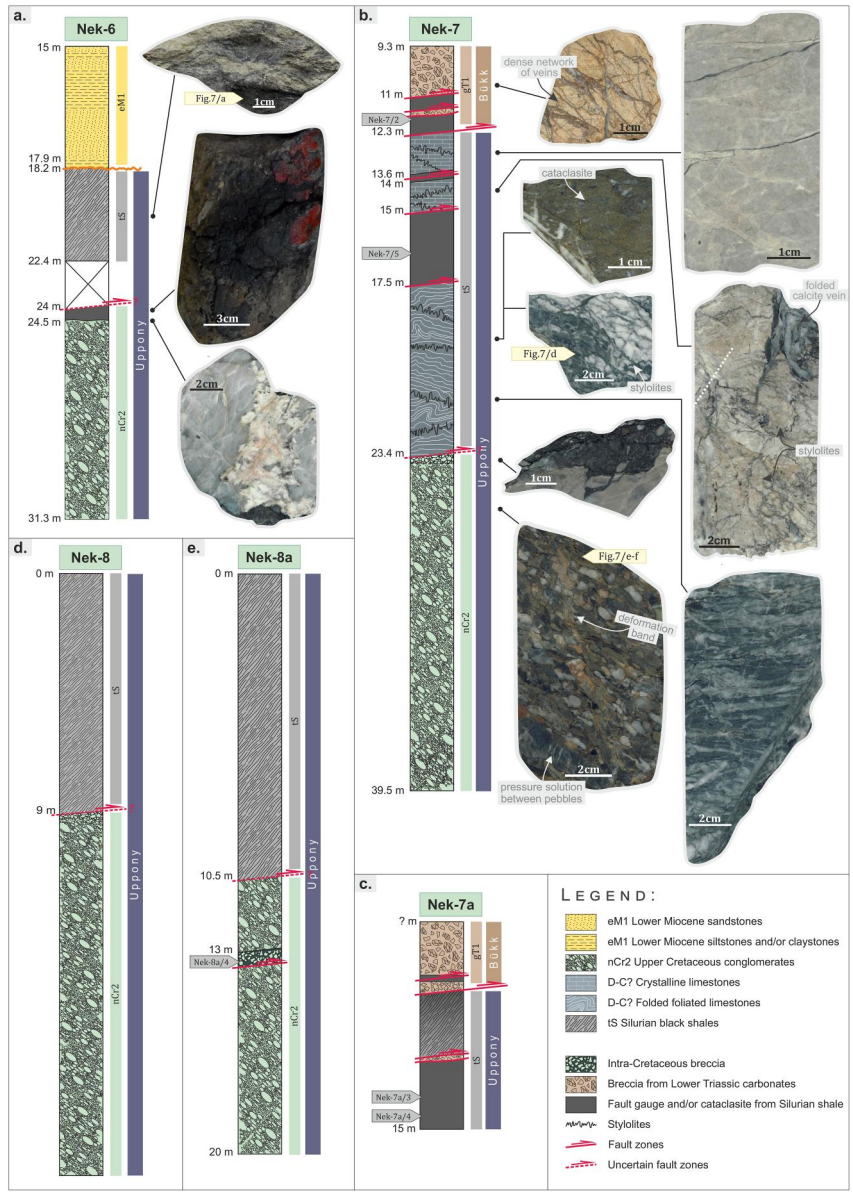

Figure 7. Revised stratigraphic columns of the analyzed boreholes: (a) Nek-6; (b) Nek-7; (c) Nek-7a; (d) Nek-8; (e) Nek-8a. The photos show the polished surfaces of the collected core samples. Note the varying thickness of the fault zone. Location of boreholes are shown in Figure 2.

5.2. Triassic Over Upper Cretaceous: Nek-7 and Nek-7a Boreholes

The Nek-7 and -7a boreholes start in a heavily fractured and metasomatized carbonatic zone (Figures 7b and 7c). The protolith of this zone cannot be determined directly due to strong alteration during deformation (Figure 8c), but its less-altered surface exposures were mapped as the lowermost Triassic carbonate (Figures 2 and 3). Downwards, this altered carbonate is replaced by a mixture of black or gray colored mixtures of claystone and siltstone. Contrary to those in the Nek-6, -8, and -8a boreholes, these sections are interpreted as fault gouges, as absolutely no foliation or any other internal structures were observed. Between the thin fault gouge sections, different types of carbonate bodies appear below 12 m depth, all of which show dynamic recrystallization and deformation twins in calcite, indicating stronger (above 250°C) alteration (Figure 8d). It is evident that this higher temperature deformation was overprinted by a low-temperature deformation that caused fracturing and rotation of foliated domains. The individual domains are surrounded by pressure solution marks. The origin of these metamorphosed carbonate bodies remains unknown as they could hardly be connected to any known formation in

10.1029/2023TC008189

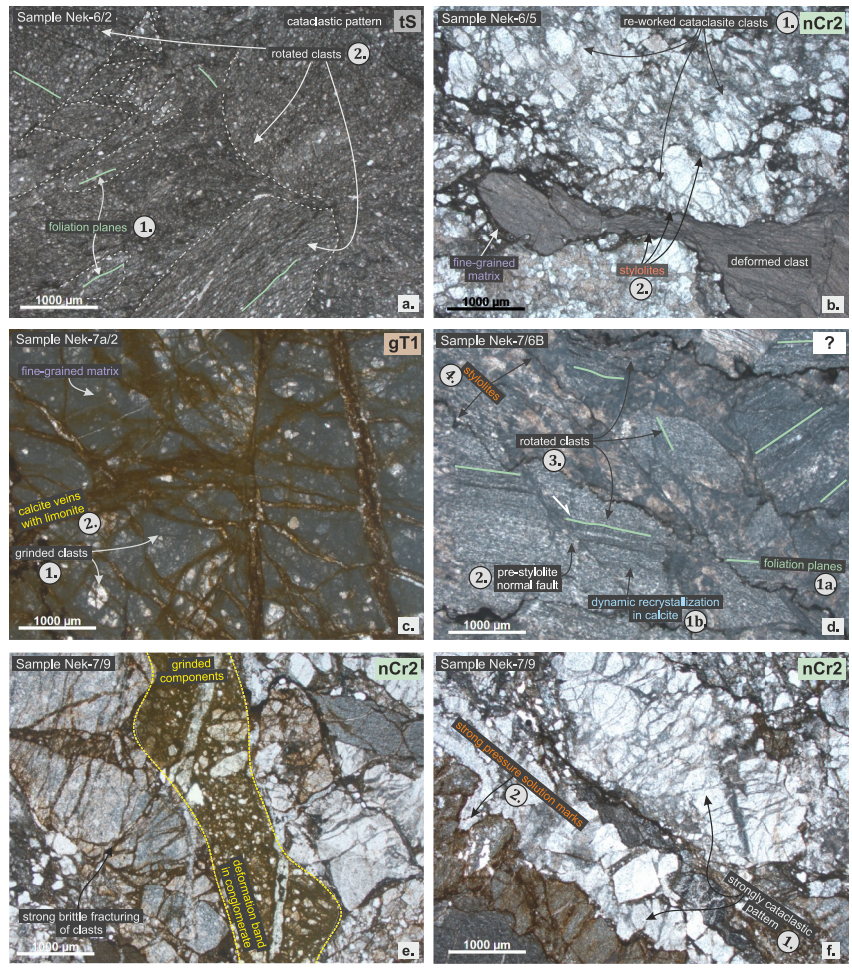

Figure 8. Interpreted microscopic images of selected core samples. Numbers refer to the relative chronological order of deformation events. (a) Characteristic cataclasite patterns in the upper black siltstone section of the Nek-6 borehole. (b) Angular clasts sitting in fine-grained matrix. Some of the larger clasts are re-worked cataclasites themselves, with pressure solution marks (stylolites) along their boundaries, suggesting strong brittle deformation prior to burial. (c) Deformed carbonate section in the Lower Triassic carbonates. (d) Dynamically re-crystallized domains with differently rotated foliation planes, indicating low-temperature deformation. Based on the pressure solution marks circling the rotated domains, burial either post-dates the low-temperature deformation. (e) Strongly fractured and grinded clasts along a deformation band in the Upper Cretaceous conglomerate. (f) Cataclastic pattern in conglomerate with post-dating pressure solution marks.

the area, but based on their metamorphic characteristics, they may be classified to some undetermined units of the UpU.

The lowermost metamorphosed carbonate is underlain by Upper Cretaceous conglomerates (Figure 7b). Its topmost part revealed a cataclastic pattern with strongly grinded components along a deformation band (Figure 8e) and firm pressure solution marks along the individual fractured domains (Figure 8f).

5.3. Interpretation of the Superposed Formations in Boreholes

The reassessed boreholes revealed the superposition of Silurian shales or Lower Triassic carbonates over the underlying Upper Cretaceous conglomerate (Figure 7; Pelikán et al., 2005; Schréter, 1953). The contact zone between them is always tectonic, even in case of the Upper Cretaceous—Silurian contacts, as the cataclastic zones and fault gouges rule out the possibility of intact overturned sedimentary contacts. In the Nek-7 borehole the tectonic zone of the NT itself is at least 23 m thick, with several internal shear zones, fault gouges and sheared blocks of fractured and metasomatized Lower Triassic carbonates on the top, and metamorphosed carbonates of

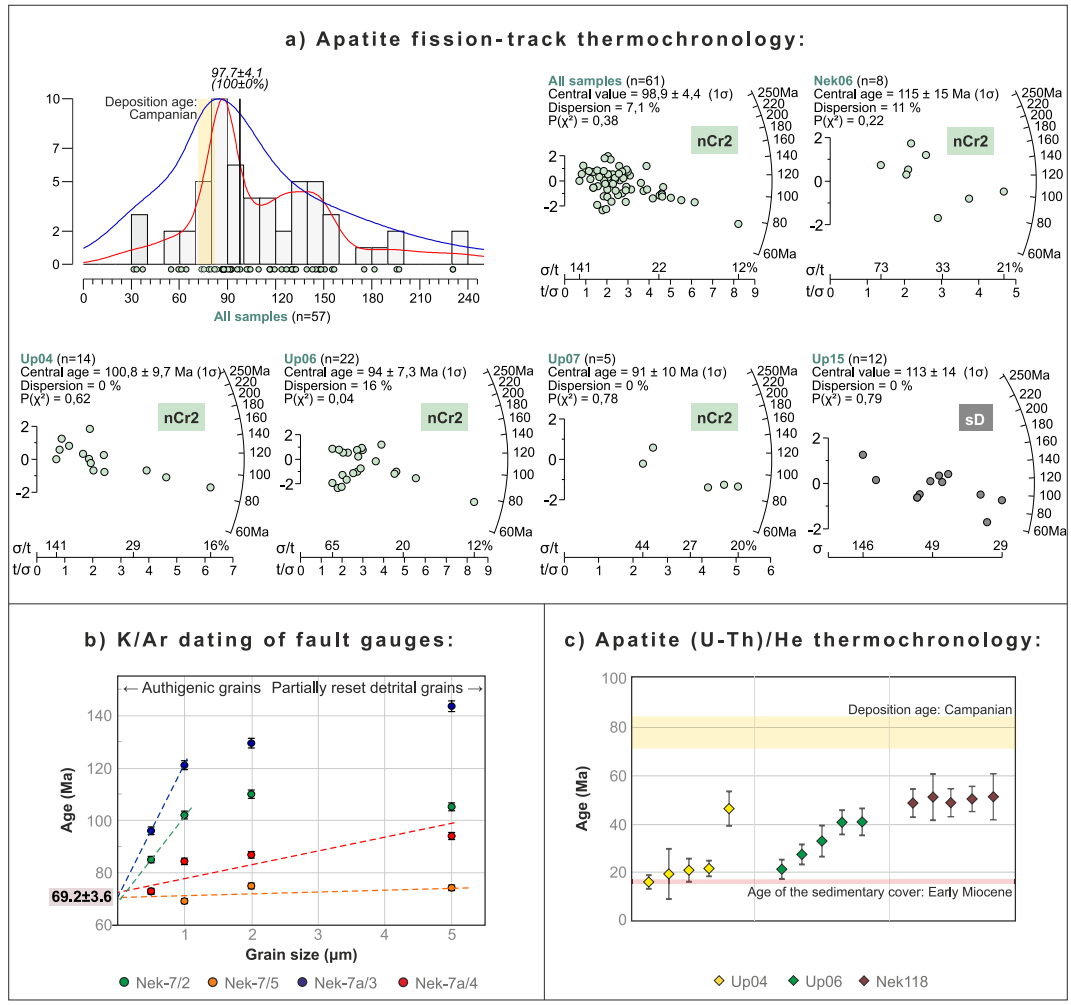

Figure 9. Summary of the thermochronology results. (a) Results of the apatite fission-track dating with respective histogram, Kernel Density Estimate (red line), Probability Density Plot (black line) and the radial plots of individual samples drawn by the RadialPlotter software (Vermeesch, 2012). See sample localities in Figure 2. (b) K/Ar dating results of fault gouge samples collected from boreholes. See sample locations in Figure 7. (c) Result of the (U-Th)/He thermochronology.

potentially UpU origin at the bottom. Penetrative cataclastic fabric in all three units indicate that the deformation along the NT took place in low-temperature conditions (even the Silurian shales deformed brittlely, Figure 8a). The pressure solution surfaces surrounding the disrupted cataclastic clasts infer that a relatively shallow burial could be associated with or follow the low-temperature deformation.

6. Thermochronology Results

6.1. Apatite Fission-Track Thermochronology

The AFT dating of the Upper Cretaceous and Devonian samples proved to be extremely challenging due to the low apatite yield of the samples, as well as the inclusion-rich nature of apatite crystals. The central ages of individual samples scatter between 91 and 116 Ma in both the Upper Cretaceous and Devonian samples (Figure 9a). Only the *Up06* sample failed the chi-square test, implying that the counted grains could derive from more than one age population. Notably, differences in the chi-square test results can be strongly influenced by the number of counted grains per sample (e.g., Vermeesch, 2012) and thus have limited meaning in the current sample set. If we consider all AFT data together, most grain ages plot between 150 and 70 Ma and yield a central age at 97.7 ± 4.1 Ma. On the summary histogram in Figure 9a, the Kernel Density Estimate of all fission-track data

imply two age components (ca. 85 and 135 Ma), however, due to the large uncertainty in the single-crystal ages, these do not necessarily have geological meaning.

6.2. K/Ar Dating of Fault Gouges

Four core samples were selected for K-Ar dating from the Nek-7, Nek-7A, and Nek-8A boreholes. Mineralogy of the selected samples were controlled by XRD analysis. Each samples contain illite, chlorite and illite/smectite in minor quantity. No quantitative analysis has been performed on the X-ray spectra in order to determine the relative quantity of the different clay minerals, but the potassium concentrations, ranging from 3.08% to 4.33% indicate that illite is the predominant phase in the samples. Quartz and potassium feldspar were absent from the samples.

All K-Ar ages obtained from the <5 μm fraction (143–75 Ma) are lower than the host Silurian slate (Figure 9b), indicating that the mica K-Ar ages were partially or completely reset during deformation-related thermal event(s). With decreasing grain size from <5 to 0.5 μm the K/Ar ages decrease in three samples and remain constant in one sample (Nek-7/5) around 70 Ma. Linear regression lines fitted on the ages of all grain size fractions (<5; <2; <1, and <0.5 μm) of the Nek-7/5 and Nek-8a/4 samples intercept the K/Ar age axis of the diagram at 69.2 ± 3.6 Ma. Linear regression with the same intercept around 69 Ma can be fitted on the fine grain size fractions (<1 and <0.5 μm) of the Nek-7/2 and Nek-7a/3 samples, but the ages of the coarse grain size fractions (<5; <2 μm) deviate from the linear trend and give relatively younger ages. Similar deviation from the linear trend in the Kongsberg silver mine and in the Kvenklubben Fault in northern Norway (Torgersen, Viola, Zwingmann, & Harris, 2015; Torgersen, Viola, Zwingmann, & Henderson, 2015) has been interpreted as an inclined age spectrum indicating combined mineral authigenesis, wall-rock comminution and fault reactivation. Multiphase reactivation is also conceivable at the study area, but the age of the earlier phases and the reactivation itself cannot be clearly demonstrated from the present data set. According to the illite age analysis method, the modeled Maastrichtian age (69.2 ± 3.6 Ma) calculated from the interception represents the termination of illite formation, that is, the time of the thrust event.

6.3. Apatite (U-Th)/He Thermochronology

Three samples contain suitable detrital apatite grains, from which 5 to 6 single-crystal aliquots were dated. The ages show significant scattering, but the unweighted means of the samples are clearly distinguishable (Figure 9c). All single-crystal ages are considerably younger than the depositional age of the dated Upper Cretaceous succession, thus a latest Cretaceous or Paleogene heating event(s) should have occurred. One possible explanation for this reheating could be the tectonic burial related to the emplacement of the BNS over the Upper Cretaceous sediments along the NT. Single grain ages range from 42 to 60 Ma for sample Nek-118 deriving from the UpU and one grain from the Upper Cretaceous Up-04. The other grains deriving from the Uppony Gosau Basin scatter between 20 and 40 Ma. The large scatter may reflect either a slow cooling through the ∼120–40°C temperature range in the Palaeogene or a complex cooling history with a heating event in the Cenozoic.

7. Discussion

7.1. Constraining the Age and Kinematics of Low Temperature Deformation Events

7.1.1. Direct Age Constraint: Fault Gouge Dating

In low temperature conditions, tectonic slip along reactivated or newly formed faults is generally associated with brittle fracturing of the host rock and progressive grain size reduction (Blenkinsop, 1991; Sibson, 1977), which ultimately results in the development of cataclasites, that is, fault breccias (Hausegger et al., 2010; Woodcock & Mort, 2008) or fault gouges (Engelder, 1974; Sammis et al., 1987), depending on the type of host rock and degree of fractionalization. As new mineral assemblages may grow or recrystallize within these fault rocks during fault slip (Niwa et al., 2016), the age of such syn-kinematic minerals reflects the age of the fault movement itself. While in carbonatic sequences the most common syn-kinematic calcite minerals can be dated by U-Pb and U-Th methods (Nuriel et al., 2012; Oren et al., 2020; Williams et al., 2019), K/Ar dating of K-rich micas, such as illite, provide the best tools for dating siliciclastic fault rocks and fault gouges (Haines & van der Pluijm, 2008; Heineke et al., 2019; Kralik et al., 1987; Mancktelow et al., 2015, 2016; Pleuger et al., 2012; van der Pluijm et al., 2001; Yamasaki et al., 2013).

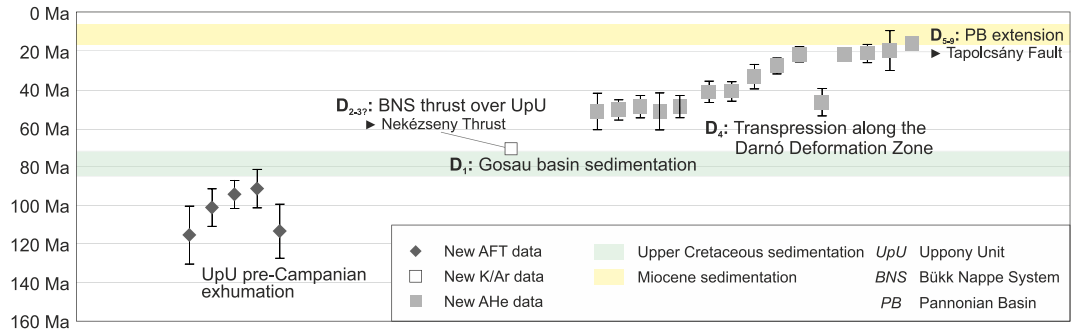

Figure 10. Summary of the new thermo-tectonic data from the Uppony Unit and their correlation to the activity of the most important structural elements in the area.

The relationship between the polytypism of dioctahedral mica (illite/muscovite), its origin (detrital or authigenic) and K/Ar age has long been known (Meunier & Velde, 2004), but dating low temperature fault gouges in general represents important challenges for geochronological studies (e.g., Bense et al., 2014; Scheiber et al., 2019). On one hand, sampling and sample preparation from fault gouges is often time consuming and requires such delicate handling that many choose to avoid using this method altogether to date fault movements. On the other hand, a high scattering and uncertainty in the acquired age is common, which is usually related to the lack of well-defined thermal events and inherited ages. Moreover, age determination is particularly challenging when illite occurs not only in the fault zone, but also in the displaced fault blocks (Scheiber et al., 2019; Torgersen, Viola, Zwingmann, & Harris, 2015; Torgersen, Viola, Zwingmann, & Henderson, 2015; Viola et al., 2016).

In this study, we successfully constrained the latest fault movements along the NT by dating fault gouge samples collected from the investigated shear zone. In our specific case, only one sample showed a uniform thrusting age and related cataclasis independently of the grain size (Nek-7/5 in Figure 9b), while in other samples the acquired ages generally increase with increasing grain size. This is due to the fact that detrital high-temperature illite/muscovite is typically coarse-grained and has $2M_1$, while newly crystallizing authigenic illite particles have a polytype of $1M_d$. With decreasing grain size, the relative amount of $1M_d$ polytype of illite increases in the various separated grain size fractions, and hence the apparent age of the fractions is decreasing. While this shows that the degree of overprinting strongly depends on the grain size and is spatially very heterogeneous even within the same fault rock unit, our results also highlight that careful grain size separation and K/Ar age determination of individual grains can enable fault activity dating. When plotting grain sizes or polytype ratios against their K/Ar age, called Illite Age Analysis, a linear relationship can be established (Pevear, 1999). It has been shown that the extrapolated K/Ar ages to zero grain size (0% $2M_1$ detrital mica) should represent the mean age of illite formation that is, the age of diagenesis, hydrothermal fluid flow or tectonic event. As the grain size and the polytype correlate linearly, the grain size-K/Ar age diagrams may also provide valuable age determinations (Garduño-Martínez et al., 2015; Zwingmann & Mancktelow, 2004; Zwingmann et al., 2010).

7.1.2. Indirect Age Constraint: Thermal History

In addition to the direct dating of fault movements via fault gouges, different low temperature thermochronology methods provide further tools for constraining the thermal evolution of displaced fault blocks. In our study, we combined AFT and AHe dating to document a deeper and shallower burial state of the investigated Late Cretaceous Uppony Gosau Basin in the footwall of the NT and at the same time, in the hanging wall of the UT (Figure 2).

As the AFT ages obtained on the Upper Cretaceous sandstone are all older than the depositional age (Figures 9a and 10), they show non- or only slightly modified memory on the pre-Campanian cooling history of the formations sourcing the sediments. As such, the AFT ages record the late Early to earliest Late Cretaceous tectonic exhumation history of the source areas of the apatite grains, with central ages of the individual samples ranging between 116 and 90 Ma. These results also provide a depth constraint over the tectonic burial related to the NT: the dated sediment could have resided only in the shallower part of the AFT partial annealing zone (Gleadow & Fitzgerald, 1987) and only for just a short time interval, which means that the thickness of the hanging wall unit (overthrust BNS) probably could not exceed 2.5–3 km.

At the same time, AHe data constrain the minimum burial (heating) of the Uppony Gosau Basin. As the AHe data acquired from the Upper Cretaceous and Devonian samples yielded He-ages ranging between 40 and 16 Ma (Figures 9c and 10), which are significantly younger than both the deposition age and the AFT ages, the temperature during the subsequent thermo-tectonic events was high enough to reset the apatite He-thermochronometer roughly around 75°C (Farley, 2002; Farley et al., 1996), while the AFT ages remained basically unaffected and are thus largely devoid of any syn- to post-thrusting signature. The results of these two dating methods put a narrow temperature constraint on the thermal evolution and imply a roughly 2.5–3 km thick tectonic overburden.

The interpretation of the individual AHe ages is multifold. On one hand, they can indicate a gradual and spatially heterogeneous cooling from the Late Eocene to Early Miocene in the footwall of the NT, uninterrupted by any deformation event. On the other hand, the cooling may also be related to deformation-induced uplift. In the next chapters, we will argue in favor of this second interpretation, namely that the new AHe-ages reflect the tectonic exhumation of the Uppony Gosau Basin in the hanging wall of the actively deforming UT.

7.1.3. Relative Age Constraints: Tilt Tests of Faults and Early Deformation Structures

Relative chronology between deformation events obtained during the fault-slip analysis can significantly contribute to the dating of deformation events. In this study, we used two approaches, that is, recognizing syn-sedimentary to syn-diagenetic fractures and applying tilt tests to determine the relative chronology of the individual fractures and related deformation phases with respect to the main folding event. Syn-sedimentary and syn-diagenetic fractures are the earliest features in the deformation history that either formed contemporaneously with the sedimentation or prior to the complete cementation of the rock. These features may be recognized for instance by the lack of discrete fault planes, thickening of the displaced beds toward the faults, faults being covered by the subsequent undeformed beds, and "plastic" rotation of the pebbles along the faults. In our study, these early fractures correspond to the normal faults of the D_1 phase (Figures 4a and 5), which seems to be roughly coeval with the Gosau basin formation.

Tilt tests applied for all sites revealed that two deformation events (D_1 and D_{2a} in Figures 4b, 4c, and 5) occurred when the bedding was still sub-horizontal, that is, prior to the main folding event (D_{2b}). In case of the pre-tilt D_1 phase, the positive tilt test was crucial in separating these early deformation features from the post-tilt discrete extensional fracture populations of the Middle to Late Miocene D_5–D_9 phases with similar fault orientations. On the other hand, the pre-tilt contractional structures of the D_{2a} phase demonstrate that shortening started at a relatively undeformed sequence and continued in a coaxial way with folding. Combination of the acquired thermochronology data with the relative order of the different deformation phases allows for a more detailed and temporally better constrained reconstruction of these low temperature deformation events.

7.2. Deformation History of the Nekézseny Thrust

7.2.1. Geometry of the Nekézseny Thrust

The NT is the structural boundary between the Austroalpine-related UpU and Dinarides-related BNS with top-to-NW tectonic transport direction (Figures 2 and 3). Based on its exposed segments, the NT has a flat-ramp-flat geometry: the low-angle to moderately dipping ramp segment runs along the eastern boundary of Nekézseny village (Figure 6a), while the sub-horizontal upper flat segment is exposed southward of the village (Figure 6b). The Miocene TF follows the ramp segment of the NT, partly displacing, partly reactivating it. Due to this extensional overprint and the Lower Miocene sedimentary cover, the ramp segment cannot be traced laterally on the surface, however, a narrow belt of Gosau sediments along the northern part of the TF also reflects the subsurface continuation of the NT ramp segment.

The minimal overall displacement of the BNS over the UpU is estimated to be around 3 km (Figure 6b). This is the perpendicular distance between the exposed ramp and the *Cso-28* and *Cso-30* boreholes, which penetrated the westernmost known occurrences of the hanging wall, that is, the BNS-type Triassic formations. However, we interpret the overturned Upper Cretaceous directly below the ramp segment of the NT as a strongly deformed and displaced very tight recumbent fold (Figure 6a). To achieve this large and tight fold geometry, the required displacement is probably much more than the minimum 3 km, implying that the NT could be a nappe boundary.

10.1029/2023TC008189

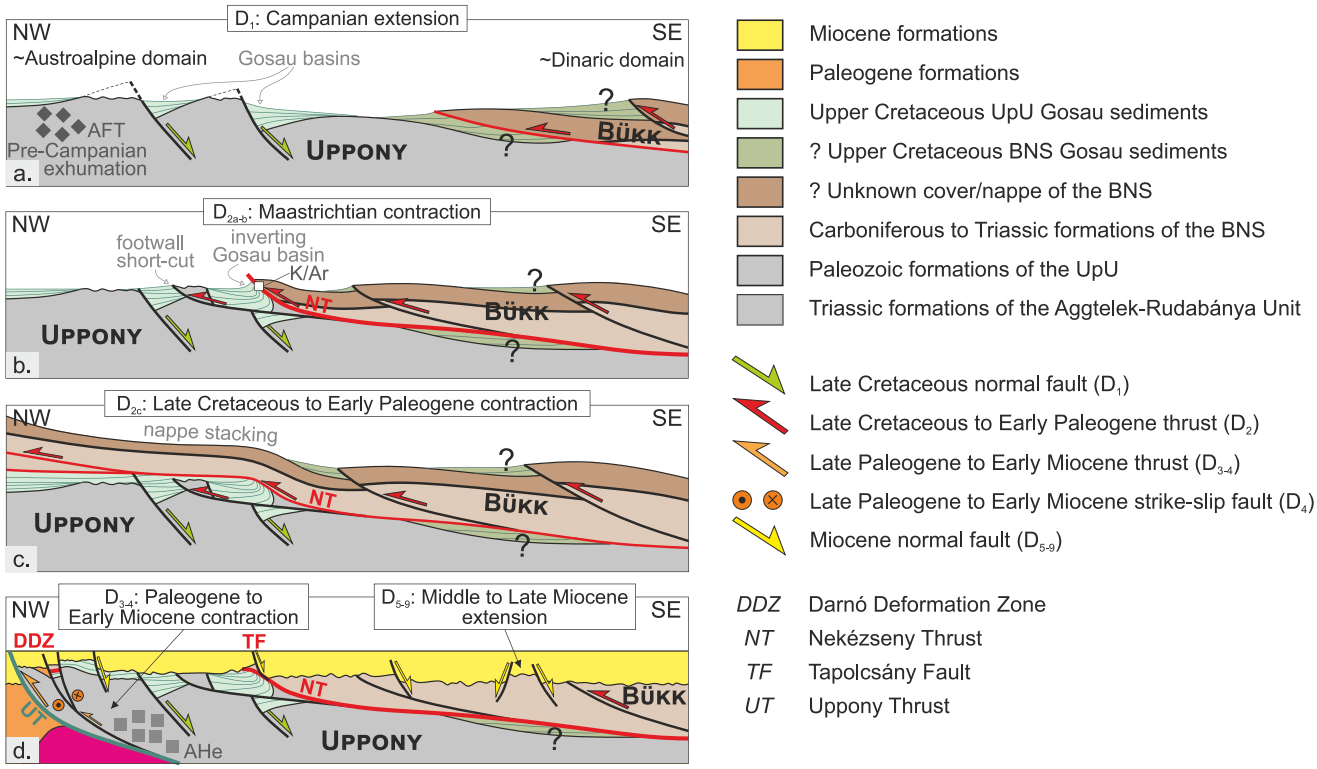

Figure 11. Schematic evolutionary model based on our observations and age data (not to scale). (a) D_1: Late Cretaceous Gosau basin formation, which was linked to normal faulting of the foreland area in front of the approaching thrust sheets. (b) D_2: Late Cretaceous underthrusting of the Gosau basin, formation of the Nekézseny Thrust, and (c) emplacement of the Bükk Nappe System over the Uppony Unit. (d) $D_{3\text{-}4}$: Further thrusting and transpressional deformation of the Bükk-Uppony area and the Darnó Deformation Zone during the Paleogene to earliest Miocene. $D_{5\text{-}9}$: Miocene normal faulting and extensional overprinting of the inherited structures during the formation of the Pannonian Basin.

7.2.2. Late Cretaceous Gosau Basin Evolution and Subsequent Thrusting

Deposition of the Upper Cretaceous (Campanian) conglomerates of the UpU records the coeval development and subsidence of the Uppony Gosau Basin (Figures 10 and 11a). The associated sedimentary slump structures (Figure 4d) and syn-diagenetic normal faults (Figures 4a and 4b) mostly indicate NE-SW striking slope and basin orientation (in present-day directions), although oblique and perpendicular early fault structures were also observed (D_1 phase, Figure 5).

Structural inversion of this Late Cretaceous basin was controlled by the arrival and NW-directed tectonic emplacement of the BNS over the UpU along the NT during the D_2 phase (Figure 11b). K/Ar dating of fault gouges collected from the NT's shear zone showed that the latest detectable fault movements occurred at around 70 Ma (Figure 10), while the shear zone itself, characterized by cataclasites, breccias and fault gouges, indicates low temperature deformation (Figures 5 and 8).

The Maastrichtian age (69.2 ± 3.6 Ma) of this deformation means that the thrusting along the NT occurred shortly after the Campanian deposition (84-72 Ma) of the Gosau sediments (Schréter, 1945; Sieglné Farkas, 1984). This correlates well with the microtectonic observations, which implied low temperature conditions and cataclasis prior to shallow burial and associated pressure solution (Figures 8b and 8f). Therefore, to explain this short time frame, the development of the Uppony Gosau Basin probably occurred in the footwall of an approaching thrust sheet as a flexural basin (Figure 11a). In this interpretation, the observed normal faulting would have occurred in the down-bending flexural foreland area (following the model of Bradley and Kidd (1991) and Doglioni (1994)), which is supported by the parallel orientation of the early extensional structures of the D_1 phase, the ramp segment of the emerging NT and other pre-tilt thrust faults of the D_{2a} phase (Figure 5). On the other hand, normal faulting oblique and perpendicular to the future NT could be explained by local stress field variations near the lateral ramps or as along-strike stretching of the footwall of the main thrust contact (Tavani et al., 2015). The occurrences

of thrust faults having been formed in sub-horizontal bed positions also show that pre-tilt thrusting was an early deformation feature, just after normal faulting.

The newly obtained AFT ages are in accordance with the previous AFT data from the UpU, they are certainly older than those determined in the adjacent BNS (typically around 55–32 Ma, Árkai et al., 1995). This data strengthens the results of pebble composition studies indicating that the clasts of the Uppony Gosau Basin do not originate from the BNS in the hanging wall of the NT, instead, the primary pebble sources were the Paleozoic bedrocks of the UpU and the non-metamorphic carbonates of some nearby units (e.g., exposed along the UT in the west, Brezsnyánszky & Haas, 1984). Other source units cannot be excluded; one example is the Upper Jurassic platform carbonate pebbles which could be derived from such a no longer preserved supra-Bükk sequence (Mišik, 1979). This and the AFT age difference have a strong implication for the NT, either indicating fast and long-distance tectonic transport of the BNS toward the UpU within a short time span in the latest Cretaceous, or the BNS was already close to the UpU during the "mid-Cretaceous," but remained buried until the Maastrichtian, that is, the end of sedimentation of the Gosau basin. This latter scenario is in agreement with Cenozoic AFT ages from BNS. In any case, the NT seems to represent a first-order tectonic contact within the orogen.

7.2.3. Paleogene to Early Miocene Thrusting and Cooling

The upper time limit for the convergence between the BNS and UpU remains poorly constrained due to the lack of Paleogene sediments in the area. As the upper Lower Miocene discordantly covers the NT and every related structure, the absolute upper age limit is the late Early Miocene, ca. 18.5 Ma (Figures 2 and 6). Unfortunately, the stress axes of the three post-tilt contractional deformation phases are very close in orientation: D_{2c} and D_4 even have the same NW-SE σ_1 axis, while the N-S σ_1 of the D_3 is also very close (Figure 5), making the separation of these deformation events hard. The similar σ_1 orientations, however, raises the possibility that the intermediate D_3 is only the result of a spatial or temporal variation of the same extended NW-SE contractional deformation, thus a continuous NW-SE oriented contraction may have taken place from the Maastrichtian till the late Early Miocene.

The obtained He-ages ranging between 16 and 40 Ma (Late Eocene to Early Miocene) corresponds well with the probable activity of the UT and the connected unroofing of the Gosau sediments in its hanging wall (Figure 6b). This fault, bounding one sub-basin of the North Hungarian Paleogene Basin from one side (Báldi & Báldi-Beke, 1985), was active during the sedimentation of the western footwall basin with continuous sedimentation, and delimits the UpU in the hanging wall with no Paleogene sedimentation. This geometry was demonstrated by seismic sections (Fodor et al., 2005; Kovács et al., 2020; Sztanó & Tari, 1993), borehole and stratigraphic data (Babinszki et al., 2023; Báldi & Báldi-Beke, 1985; Less et al., 2006; Szentpétery, 1988; Telegdi Roth, 1951). The reverse kinematics is additionally supported by fault-slip data (Beke et al., 2021; Fodor et al., 2005; Petrik et al., 2016), while sedimentary features and deformation bands of Early Miocene age refer to a short period of sinistral transpression (Beke et al., 2019; Sztanó & Józsa, 1996). This independent argument favors the cooling of the UpU registered by the apatite He-ages during the thrusting along the UT.

7.2.4. Late Early to Early Late Miocene Extensional Deformation

Lastly, the juxtaposed BNS and UpU were affected by extensional faulting during the late Early to early Late Miocene formation of the Pannonian Basin ($D_{5\text{-}9}$ phases, Figure 5; Beke et al., 2019, 2021; Fodor et al., 2005; Petrik et al., 2016). This led to the formation of the TF and extensional overprinting of the NT (Figure 11d).

7.3. Similar Low Temperature Deformation Features in the UpU and BNS

Our results show that the NT is a NW-vergent Maastrichtian nappe boundary between the UpU and BNS. This N- and NW-directed tectonic transport is widespread in the whole UpU, with most of these contractional structures being related to the Early Cretaceous prograde stage of the Eoalpine orogeny (Figure 6; Csontos, 1999; Koroknai, 2004; Schréter, 1943). However, Koroknai (2004) also recognized locally present late-stage crenulation cleavage with both NW- and SE-directed shearing, as well as even younger kink folds with steep axial planes along the dominantly NW-SE striking shear zones.

In contrast, in the hanging wall of the NT, in the BNS, the most penetrative contractional deformation is the south to southeast vergent overturned folds and related axial plane foliation (Csontos, 1999). However, Csontos (1999), McIntosh (2014), and Juhász et al. (2021) observed NW-vergent reverse faults, thrusts and map-scale folds in the

Paleozoic and Lower Triassic formations of the northwestern Bükk, post-dating the general S-SE-vergent. There are further WNW-ESE striking mylonitic shear zones with the estimated deformation temperature around 260 ± 20°C in the eastern Bükk with oblique dextral strike-slip kinematics (Csontos, 1988, 1999; Koroknai et al., 2008). The ductile shearing occurred along the pre-existing axial plane foliation planes, thus this dextral faulting also represents a younger deformation phase. Additional northwestward verging structures were observed in the SW Bükk, where Scherman (2018) and Fialowski (2018) described brittle kink folds that post-dated ductile structures.

Somewhat analogs structures were also identified in the easternmost outcrop of the Transdanubian Range Unit (Figure 1a), where imbrication of Mesozoic rocks, including Upper Cretaceous (Campanian) formations were documented in the Csővár area (Haas et al., 1997). These thrusts could have formed in the same N-S contraction, albeit the vergency was just the opposite, to the south (Benkő & Fodor, 2002).

All these observations seem to confirm that there is a regionally important, low temperature NW-SE (or N-S) compressional phase with north(west)ward tectonic transport direction in the whole UpU and BNS area during the late-stage evolution of the Eoalpine orogeny. Although these structures overprint the main Late Jurassic to Early Cretaceous nappe stacking, thrusting and folding, more accurate age data have not been available before. Based on paleomagnetic data (Márton & Márton, 1996), Csontos (1999) tentatively dated the mylonitic shear zones, the south-dipping reverse faults in the central Bükk and the precursory of the Darnó Deformation Zone to the Late Cretaceous or Early Paleogene. However, Csontos (1999) debated that the subsidence of the Uppony Gosau Basin and the uplift of the central Bükk, constrained by the earlier K/Ar ages and zircon fission-track cooling ages between 95 and 80 Ma (Árkai et al., 1995), could be associated with the thrusting along these structures, but its relationship to the NT remained ambiguous. Later, Koroknai et al. (2008) dates one of the mentioned mylonitic shear zones, and K/Ar dating of K-rich micas yielded the same 75–85 Ma age for both the shear zone and the surrounding host rocks. This implied that the age of this low temperature deformation is post-75 Ma, which is in agreement with our new 69.2 ± 3.6 Ma K/Ar age for the NT. These considerations show that the shortening between the BNS and UpU was already ongoing within the BNS by the Gosau sedimentation. An even earlier initiation of this top-to-NW tectonic transport, for example, during the onset of Gosau basin formation can be supported by the acceptance of the contractional origin of the basin itself, however, this would require further geochronological constraints from the BNS. During the Maastrichtian, the gradual northward propagation of the thrust front reached our study area in the form of the NT.

7.4. Regional Implications for the Alpine-Carpathian-Dinaric Tectonic Evolution

7.4.1. Implications for the ALCAPA Unit

The Maastrichtian age of thrusting along the NT confirms that the northwestern boundary of the BNS toward the UpU is a Mesozoic structural boundary. Therefore, the BNS was already attached to other sub-units of the ALCAPA Unit by the end of the Late Cretaceous (Figure 12a; Balla, 1984; Csontos & Vörös, 2004). If there was pre-Campanian thrusting along the NT, the BNS-UpU contact could be even older. While the NT itself, and its postulated continuation along the eastern BNS, is cut by the Miocene MHSZ (Figure 12b), it is a displaced Late Cretaceous segment of the contact zone between the former Dinaric and Austroalpine domains. The estimated amount of shortening along the NT suggests that this contact could have been a latest Cretaceous nappe boundary along which the entire BNS of Dinaridic origin is thrust over the Austroalpine Inner Western Carpathian units.

7.4.2. Switching From Lower Plate to Upper Plate Between Two Oppositely Verging Subduction System

After retro-deforming the Cenozoic displacements and rotational movements along the MHSZ (Csontos & Vörös, 2004; Márton & Márton, 1996; Márton et al., 2002; Tari, 1995; Tomljenović et al., 2008), one arrives at a very complex Late Cretaceous to early Paleogene plate tectonic configuration (Figure 12a).

The investigated BNS occupies the northeastern corner of the Adriatic microplate (van Hinsbergen et al., 2020), in close vicinity of the Medvednica Mts (Figure 1a; van Gelder et al., 2015). This part of Adria had already been accreted, while the active accretion was toward the southwest, where it involved more external parts of the Dinaridic nappe system. However, this hinterland area was again/still undergoing shortening due to the closure of the Sava Ocean to the east (Pamić et al., 2002; Ustaszewski et al., 2009). From this point of view, the BNS was in lower plate position with respect to the Sava Suture and the Europe-derived Tisza microplate (van Hinsbergen

10.1029/2023TC008189

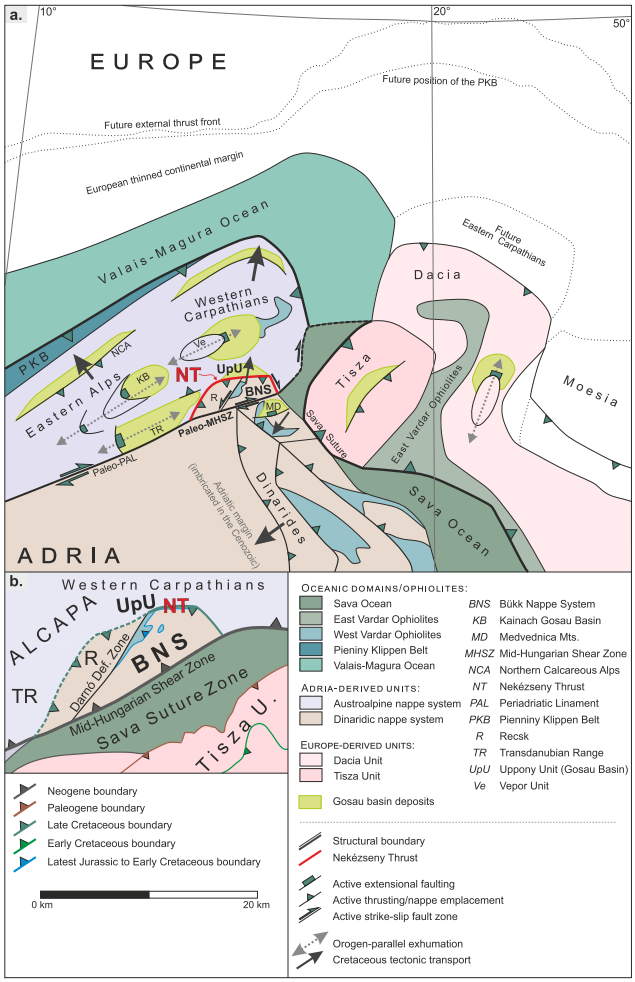

Figure 12. (a) Latest Cretaceous (~80 Ma) tectonic reconstruction of the Alpine-Carpathian-Dinaric area (modified after van Hinsbergen et al. (2020)), showing the restored position of the ALCAPA-Dinarides structural contact zone, including the Nekézseny Thrust. The Late Cretaceous Gosau basins and their tectonic character are shown schematically (after Neubauer et al. (1995), Ortner (2001), Plašienka and Soták (2015), Tari (1994), and Willingshofer et al. (1999)). (b) Tectonic map of the Bükk-Uppony area based on our new results. In our interpretation, the Nekézseny Thrust is a segment of the Maastrichtian nappe contact between the Dinarides-related Bükk Nappe System and the Austroalpine Uppony Unit. Note the Dinarides-derived unit west of the Darnó Deformation Zone (Recsk Unit, Fodor et al., 2017).

et al., 2020). The onset of collision along the Sava Suture was dated to the Maastrichtian and led to thrusting and out-of-sequence nappe emplacement until the late Eocene (Schmid et al., 2008; Ustaszewski et al., 2010). In the once-nearby Medvednica Mts., this is evidenced by large-offset thrust faults that are associated with cataclastic deformation and emplace shallow marine Triassic sequences over Upper Cretaceous to Paleogene Gosau sediments (Tomljenovič et al., 2008; van Gelder et al., 2015). Even though these structural features show striking similarities to our observations in the BNS-UpU, which means that the NT could be interpreted as the result of the collisional and post-collisional deformation of the Sava Zone, there is still a significant difference between the BNS-UpU and the Medvednica, and that is the opposite polarity of the tectonic transport direction. After retro-deforming the Cenozoic rotations (Márton & Márton, 1996; Márton et al., 2002; Tomljenovič et al., 2008), the tectonic transport direction is top-to-SW in the Medvednica and top-to-NNE in the BNS-UpU (Figure 12). This means that while the Medvednica still followed the general tectonic trend of the Dinarides, that is, it was indeed part of the imbricating Adriatic lower plate with respect to the Sava Suture, the NE-vergent NT was either a back-thrust or its vergency was controlled by some other tectonic process.

Our new results show that the BNS and the uppermost sheets of the Austroalpine nappe system (UpU) were already in direct contact along the NT by the end of the Cretaceous, which also suggests that this tectonic unit, formerly part of the northernmost segment of the Dinaridic orogen, also participated in the latest stage of the Eoalpine orogenic evolution. From this perspective, the BNS was in upper plate position with respect to the Austroalpine high pressure belt that resulted from the preceding intra-continental subduction and collision of the Austroalpine units (Frisch et al., 1998; Handy et al., 2010; Janák et al., 2004, 2015; Neubauer et al., 1999; Ratschbacher et al., 2004; Schuster et al., 2013; Stüwe & Schuster, 2010), therefore it may be considered part of the Austroalpine nappe stack within the Western Carpathians (Plašienka, 2018; Plašienka et al., 1997).

During the Late Cretaceous, the evolution of the Austroalpine domain was controlled by two main processes. On one hand, the high pressure units became subject to rapid exhumation from ca. 90 Ma onward in both the Eastern Alps and Western Carpathians (Figure 12a; Dallmeyer et al., 1996, 1998; Janák et al., 2001; Jeřábek et al., 2008; Koroknai et al., 1999; Maluski et al., 1993; Neubauer et al., 1995; Schmid et al., 2004; Thöni, 1999; Vojtko et al., 2016). This exhumation partly resulted in the formation of detachment shear zones and Late Cretaceous syn-kinematic basins in the hanging wall (Figure 12a). At the same time, as the contractional deformation gradually migrated toward the northern foreland, subduction initiation occurred in the Alpine Tethys realm in the Late Cretaceous (South Penninic Ocean, Froitzheim et al., 2008; Schmid et al., 2008; Schuster et al., 2013; Plašienka, 2018). Part of the Late Cretaceous basins could be connected to this deformation, mainly in the Northern Calcareous Alps (Ortner, 2001; Plašienka & Soták, 2015; Wagreich, 1995), but also in the Transdanubian Range (Tari, 1994; Tari & Linzer, 2018). As a result, the main location of the north to northeast vergent nappe accretion was transferred from the Austroalpine basement nappes to the Pieniny Klippen Belt in the Western Carpathians (Figure 12a; Plašienka & Mikuš, 2010; Plašienka & Soták, 2015) and to the external front of the Lower Austroalpine domain in the Alps (Froiztheim et al., 2008). However, the rest of the Western Carpathians (the southern hinterland) remained continuously affected by NNW-SSE to NE-SW directed shortening. After back-rotating the structures, the original tectonic transport direction seems to be top-to-NNE in the Western Carpathians. Considering the age and tectonic transport direction of the thrusting along the NT, we connect it to the late-stage deformation history of the Alpine-Carpathian domain, and propose that the Dinarides-related BNS was thrust over the Austroalpine nappe system as

a top-to-NNE vergent out-of-sequence thrust (Figure 12).7.4.3 Possible implications for the latest Cretaceous to early Paleogene movements along the paleo-Periadriatic Line.

As shown in the previous chapter, the latest Cretaceous to earliest Paleogene tectonic transport directions show opposite polarities in the Dinarides and Sava Zone versus BNS-UpU and Western Carpathian systems (top-to-SW and top-to-NE, respectively, according to the back-rotated directions, Figure 12a). This kinematic contradiction can be explained by taking into account the possible role of the combined Periadriatic-MHSZ. In agreement with the postulation of Handy et al. (2015) and Ustaszewski et al. (2008), it could have already separated the Dinaridic nappe system and the BNS–Austroalpine domains at this time, possibly transferring the deformation and accommodating the polarity change between the west-vergent Sava Zone and the north- and northeast-directed Pieniny Klippen Belt sutures. Late Cretaceous movements along the Periadriatic-MHSZ would also explain the contradiction between the present-day distance of the Mesozoic facies belts and the supposed amount of Late Oligocene to Early Miocene displacement along the shear zone: the distance for the Mesozoic facies markers across the shear zone is far larger than for the Cenozoic ones, with the former estimated to be around 500 km (Haas et al., 1995) and the latter to 290–350 km (Tari, 1994; Tari et al., 1995). The minimum 150 km difference could be attributed to this Late Cretaceous slip along the shear zone.

8. Conclusions

Detailed mesoscopic structural analysis and systematic low temperature thermochronological investigation were carried out near the Nekézseny Thrust to understand the thermo-tectonic evolution of the boundary area of the Austroalpine Inner Western Carpathians and the Dinaric Bükk Nappe System. Our results highlight that a combined structural and thermochronological approach may provide sufficient age, kinematic and thermal constraints to reconstruct the deformation history during several successive low temperature deformation events, even in poor outcrop conditions and large stratigraphic hiatuses. The structural analysis revealed that the Uppony Gosau basin probably formed in the footwall of the approaching thrust sheet of the Bükk Nappe System and underwent contractional deformation shortly after the deposition of the Upper Cretaceous Gosau formation, during the tectonic emplacement of the Bükk Nappe System onto the Uppony Gosau Basin. This emplacement marks the most important change in the history of this northernmost segment of the Dinaric nappe system: from the lower plate tectonic position with respect to the Sava Suture to the upper plate position with respect to the Alpine Eoalpine high pressure belt. As a result, the earlier top-to-SW tectonic transport direction changed to top-to-NE, which can be either a back-thrust in the relation of the Dinarides or rather more likely an out-of-sequence forethrust in the Austroalpine nappe-pile. K/Ar dating of fault gouges collected from the main Nekézseny Thrust nappe boundary yielded Maastrichtian age (69–70 Ma) for this thrusting event. This demonstrates that the Nekézseny Thrust is a Late Cretaceous nappe boundary between the former Austroalpine and Dinaric domains, which was displaced by the Mid Hungarian Shear Zone during the Late Oligocene to Early Miocene. Therefore, the Bükk Nappe System forms an internal part of the Miocene ALCAPA Unit. The observed cataclasites and fault gouges along the nappe boundary, as well as the lack of reset on the apatite fission tracks in the Upper Cretaceous sandstones indicate low temperature (below 100°C) deformation and shallow tectonic burial. The apatite (U-Th)/He thermochronology suggests gradual cooling between 40 and 16 Ma, and constrains the maximum temperature during the post-Campanian contractional deformation phases roughly between 75 and 100°C. Following the Oligocene to Early Miocene displacement of the Nekézseny Thrust during the lateral extrusion of the ALCAPA, the Uppony and Bükk area was affected by extensional deformation during the development of the Pannonian Basin, which led to extensional reactivation and overprint of the inherited contractional structures.

Data Availability Statement

Detailed lists of the referenced outcrop and sample localities, as well as all the measured thermochronology data are available in an open access repository (Oravecz, 2023). Stereoplots were plotted by using the analytical method of Angelier (1990).

Acknowledgments
This research was supported by the research funds NKFIH OTKA 113013, 134873, and the ÚNKP-17-2 and ÚNKP-20-3 New National Excellence Program of the Ministry of Human Capacities. The authors thank Orsolya Sztanó for the discussions on the sedimentological interpretation of the Upper Cretaceous conglomerates. Access to the borehole database was provided by the Supervisory Authority for Regulatory Affairs of Hungary.

References

Angelier, J. (1984). Tectonic analysis of fault slip data sets. *Journal of Geophysical Research*, *89*(B7), 5835–5848. https://doi.org/10.1029/JB089iB07p05835

Angelier, J. (1990). Inversion of field data in fault tectonics to obtain the regional stress—III. A new rapid direct inversion method by analytical means. *Journal of Geophysical Research*, *103*(2), 363–376. https://doi.org/10.1111/j.1365-246x.1990.tb01777.x

Árkai, P., Balogh, K., & Dunkl, I. (1995). Timing of low-temperature metamorphism and cooling of the Paleozoic and Mesozoic formations of the Bükkium, innermost Western Carpathians, Hungary. *Geologische Rundschau*, *84*(2), 334–344. https://doi.org/10.1007/s005310050009

Babinszki, E., Piros, O., Csillag, G., Fodor, L., Gyalog, L., Kercsmár, Z., et al. (2023). Lithostratigraphy of Hungary II. Cenozoic formations. *Szabályozott Tevékenységek Felügyeleti Hatósága, Budapest*, 15–51.

Balázs, A., Matenco, L., Magyar, I., Horváth, F., & Cloetingh, S. (2016). The link between tectonics and sedimentation in back-arc basins: New genetic constraints from the analysis of the Pannonian Basin. *Tectonics*, *35*(6), 1526–1559. https://doi.org/10.1002/2015tc004109

Báldi, T., & Báldi-Beke, M. (1985). The evolution of the Hungarian Paleogene basins. *Acta Geologica Hungarica*, *28*, 5–28.

Balla, Z. (1983). Development of the Pannonian basin basement through the Cretaceous-Cenozoic collision: A new synthesis. *Tectonophysics*, *88*(1–2), 61–102. https://doi.org/10.1016/0040-1951(82)90203-7

Balla, Z. (1984). The Carpathian loop and the Pannonian basin: A kinematic analysis. *Geophysical Transactions*, *30*(4), 313–353.

Balla, Z. (1986). Palaeotectonic reconstruction of the central Alpine-Mediterranean belt for the Neogene. *Tectonophysics*, *127*(3), 213–243. https://doi.org/10.1016/0040-1951(86)90062-4

Balla, Z. (1988). Clockwise paleomagnetic rotations in the Alps in the light of the structural pattern of the Transdanubian Range (Hungary). *Tectonophysics*, *145*(3–4), 277–292. https://doi.org/10.1016/0040-1951(88)90200-4

Balogh, K. (1964). A Bükkhegység földtani képződményei (Die geologischen Bildungen des Bükk-gebirges). *Magyar Allami Foldtani Intezet Evkonyve*, *48*(2), 558–713.

Beke, B., Fodor, L., Millar, L., & Petrik, A. (2019). Deformation band formation as a function of progressive burial: Depth calibration and mechanism change in the Pannonian Basin (Hungary). *Marine and Petroleum Geology*, *105*, 1–16. https://doi.org/10.1016/j.marpetgeo.2019.04.006

Beke, B., Szőcs, E., Hips, K., Schubert, F., Petrik, A., Milovský, R., & Fodor, L. (2021). Evolution of deformation mechanism and fluid flow in two pre-rift siliciclastic deposits (Pannonian Basin, Hungary). *Global and Planetary Change*, *199*, 103434. https://doi.org/10.1016/j.gloplacha.2021.103434

Benkő, K., & Fodor, L. (2002). Structural geology near Csővár, Hungary. *Foldtani Kozlony*, *132*(2), 223–246.

Bense, F. A., Wemmer, K., Löbens, S., & Siegesmund, S. (2014). Fault gouge analyses: K–Ar illite dating, clay mineralogy and tectonic significance—A study from the Sierras Pampeanas, Argentina. *International Journal of Earth Sciences*, *103*(1), 189–218. https://doi.org/10.1007/s00531-013-0956-7

Blenkinsop, T. G. (1991). Cataclasis and process of particle size reduction. *Pure and Applied Geophysics*, *136*(1), 59–86. https://doi.org/10.1007/bf00878888

Bradley, D. C., & Kidd, W. S. F. (1991). Flexural extension of the upper continental crust in collisional foredeeps. *Geological Society of America Bulletin*, *103*(11), 1416–1438. https://doi.org/10.1130/0016-7606(1991)103<1416:feotuc>2.3.co;2

Brezsnyánszky, K., & Haas, J. (1984). The Nekézseny conglomerate formation of Senonian age: A sedimentological and tectonic study of the stratotype section. *Foldtani Kozlony*, *114*, 81–100.

Carrera, N., & Munoz, J. A. (2008). Thrusting evolution in the southern Cordillera Oriental (northern Argentine Andes): Constraints from growth strata. *Tectonophysics*, *459*(1–4), 107–122. https://doi.org/10.1016/j.tecto.2007.11.068

Channell, J. E. T., D'Argenio, B., & Horváth, F. (1979). Adria, the African promontory in Mesozoic Mediterranean paleogeography. *Earth-Science Reviews*, *15*(3), 213–292. https://doi.org/10.1016/0012-8252(79)90083-7

Clifton, H. E., Brezsnyánszky, K., & Haas, J. (1985). Lithologic characteristics and paleogeographic significance of resedimented conglomerate of Late Cretaceous age in Northern Hungary. *Geophysical Transactions*, *31*(1–3), 131–155.

Csontos, L. (1988). Étude géologique d'une portion des Carpathes internes: le massif du Bükk (Nord-Est de la Hongrie): Stratigraphie, structures, métamorphisme et géodynamique. PhD thesis. Université de Lille Flandres-Artois.

Csontos, L. (1995). Tertiary tectonic evolution of the Intra-Carpathian area: A review. *Acta Vulcanologica*, *7*, 1–13.

Csontos, L. (1999). Structural outline of the Bükk Mts (N Hungary). *Foldtani Kozlony*, *129*(4), 611–651.

Csontos, L. (2000). Stratigraphic reevaluation of the Bükk Mts (N. Hungary). *Foldtani Kozlony*, *130*(1), 95–131.

Csontos, L., & Nagymarosy, A. (1998). The mid-Hungarian line: A zone of repeated tectonic inversions. *Tectonophysics*, *297*(1–4), 51–71. https://doi.org/10.1016/s0040-1951(98)00163-2

Csontos, L., Nagymarosy, A., Horváth, F., & Kováč, M. (1992). Tertiary evolution of the Intra-Carpathian area: A model. *Tectonophysics*, *208*(1–3), 221–241. https://doi.org/10.1016/0040-1951(92)90346-8

Csontos, L., & Vörös, A. (2004). Mesozoic plate tectonic reconstruction of the Carpathian region. *Paleogeography, Paleoclimatology, Paleoecology*, *210*, 1–56. https://doi.org/10.1016/j.palaeo.2004.02.033

Dallmeyer, R. D., Handler, R., Neubauer, F., & Fritz, H. (1998). Sequence of thrusting within a thick-skinned tectonic wedge: Evidence from $^{40}Ar/^{39}Ar$ and Rb-Sr ages from the Austroalpine Nappe Complex of the Eastern Alps. *The Journal of Geology*, *106*(1), 71–86. https://doi.org/10.1086/516008

Dallmeyer, R. D., Neubauer, F., Handler, R., Fritz, H., Müller, W., Pana, D., & Putiš, M. (1996). Tectonothermal evolution of the internal Alps and Carpathians: Evidence from $^{40}Ar/^{39}Ar$ mineral and whole-rock data. *Eclogae Geologicae Helvetiae*, *89*(1), 203–227.

DeCelles, P. G., Lawton, T. F., & Mitra, G. (1995). Thrust timing, growth of structural culminations, and synorogenic sedimentation in the type Sevier orogenic belt, western United States. *Geology*, *23*(8), 699–702. https://doi.org/10.1130/0091-7613(1995)023<0699:ttgosc>2.3.co;2

Dimitrijević, M. D., & Dimitrijević, M. N. (1973). Olistostrome mélange in the Yugoslavian Dinarides and Late Mesozoic plate tectonics. *The Journal of Geology*, *81*(3), 328–340. https://doi.org/10.1086/627874

Doglioni, C. (1994). Geological remarks on the relationships between extension and convergent geodynamic settings. *Tectonophysics*, *252*(1–4), 253–267. https://doi.org/10.1016/0040-1951(95)00087-9

Dumitru, T. A. (1993). A new computer-automated microscope stage system for fission-track analysis. *Nuclear Tracks and Radiation Measurements*, *21*(4), 575–580. https://doi.org/10.1016/1359-0189(93)90198-i

Dunkl, I. (2002). Trackkey: A windows program for calculation and graphical presentation of fission track data. *Computational Geosciences*, *28*(1), 3–12. https://doi.org/10.1016/s0098-3004(01)00024-3

Engelder, J. T. (1974). Cataclasis and the generation of fault gouge. *Geological Society of America Bulletin*, *85*(10), 1515–1522. https://doi.org/10.1130/0016-7606(1974)85<1515:catgof>2.0.co;2

Farley, K. A. (2002). (U-Th)/He dating: Techniques, calibrations, and applications. *Reviews in Mineralogy and Geochemistry*, *47*(1), 819–844. https://doi.org/10.2138/rmg.2002.47.18

Farley, K. A., Wolf, R. A., & Silver, L. T. (1996). The effects of long alpha-stopping distance on (U-Th)/He ages. *Geochimica et Cosmochimica Acta*, *60*(21), 4223–4229. https://doi.org/10.1016/s0016-7037(96)00193-7

Fialowski, M. (2018). Deformation and kinematics of the Mónosbél Nappe, Bátor area, SW Bükk. MSc thesis. Eötvös Loránd University.

Fodor, L., Csontos, L., Bada, G., Györfi, I., & Benkovics, L. (1999). Tertiary tectonic evolution of the Pannonian Basin system and neighboring orogens: A new synthesis of palaeostress data. In B. Durand, L. Jolivet, F. Horváth, & M. Séranne (Eds.), *The Mediterranean basins: Tertiary extension within the Alpine Orogen* (Vol. 156, pp. 295–334). Geological Society Special Publications.

Fodor, L., Héja, G., Kövér, S., Csillag, G., & Csicsek, Á. (2017). Cretaceous deformation of the south-eastern Transdanubian Range Unit, and the effect of inherited Triassic-Jurassic normal faults. In S. Kövér, & L. Fodor (Eds.), *15th meeting of the central European tectonic studies group (CETeG), Acta Mineralogica-Petrographica, field guide series* (Vol. 93, pp. 30–31).

Fodor, L., Jelen, B., Márton, E., Skaberne, D., Čar, J., & Vrabec, M. (1998). Miocene-Pliocene tectonic evolution of the Slovenian Periadriatic fault: Implications for Alpine-Carpathian extrusion models. *Tectonics*, *17*(5), 690–709. https://doi.org/10.1029/98tc01605

Fodor, L., Oravecz, É., Less, G., & Kövér, S. (2023). Structure and evolution of the Aggtelek and Rudabánya Hills, NE Hungary. In *Pre- and post-conference field trip guide book, 19th meeting of the central European tectonic studies group, Kazincbarcika. Acta Mineralogica-Petrographica field guide series* (Vol. 34, pp. 1–68).

Fodor, L., Radócz, G., Sztanó, O., Koroknai, B., Csontos, L., & Harangi, S. (2005). Post-conference excursion: Tectonics, sedimentation and magmatism along the Darnó Zone. *Geolines*, *19*, 141–161.

Fodor, L., Sztanó, O., Csontos, L., Józsa, S., & Nagymarosy, A. (1992). *Tectonic and sedimentological research in the Darnó Zone near the Darnó Hill and Uppony Mts. Manuscript*. Geological Institute of Hungary and Eötvös Loránd University of Sciences.

Folguera, A., Bottesi, G., Dubby, I., Martín-González, F., Orts, D., Sagripanti, L., et al. (2015). Exhumation of the Neuquén Basin in the southern Central Andes (Malargüe fold and thrust belt) from field data and low-temperature thermochronology. *Journal of South American Earth Sciences*, *64*(2), 381–398. https://doi.org/10.1016/j.jsames.2015.08.003

Frisch, W., Kuhlemann, J., Dunkl, I., & Brügel, A. (1998). Palinspastic reconstruction and topographic evolution of the Eastern Alps during late Tertiary tectonic extrusion. *Tectonophysics*, *297*(1–4), 1–15. https://doi.org/10.1016/s0040-1951(98)00160-7

Froitzheim, N., Plašienka, D., & Schuster, R. (2008). Alpine tectonics of the Alps and western Carpathians. In T. McCann (Ed.), *The geology of central Europe, Mesozoic and Cenozoic* (Vol. 2, pp. 1141–1232). Geological Society Publishing House.

Fügenschuh, B., Mancktelow, N. S., & Seward, D. (2000). Cretaceous to Neogene cooling and exhumation history of the Oetztal-Stubai basement complex, Eastern Alps: A structural and fission track study. *Tectonics*, *19*(5), 905–918. https://doi.org/10.1029/2000tc900014

Galbraith, R. F., & Laslett, G. M. (1993). Statistical models for mixed fission track ages. *Nucklear Tracks and Radiation Measurements*, *21*(4), 459–470. https://doi.org/10.1016/1359-0189(93)90185-c

Garduño-Martínez, D. E., Pi Puig, T., Solé, J., Martini, M., & Alcalá-Martínez, J. R. (2015). K-Ar illite-mica age constraints on the formation and reactivation history of the El Doctor fault zone, central Mexico. *Revista Mexicana de Ciencias Geológicas*, *32*, 306–322.

Gleadow, A. J. W. (1981). Fission-track dating methods: What are the real alternatives? *Nucklear Tracks*, *5*(1–2), 3–14. https://doi.org/10.1016/0191-278x(81)90021-4

Gleadow, A. J. W., & Fitzgerald, P. G. (1987). Uplift history and structure of the Transantarctic Mountains: New evidence from fission track dating of basement apatites in the Dry Valleys area, southern Victoria Land. *Earth and Planetary Science Letters*, *82*(1–2), 1–14. https://doi.org/10.1016/0012-821x(87)90102-6

Haas, J., Budai, T., Csontos, L., Fodor, L., & Konrád, G. (2010). *Pre-Cenozoic geological map of Hungary*. Geological Institute of Hungary.

Haas, J., & Kovács, S. (2001). The Dinaridic-Alpine connection—As seen from Hungary. *Acta Geologica Hungarica*, *44*(2–3), 345–363.

Haas, J., Kovács, S., Krystyn, L., & Lein, R. (1995). Significance of Late Permian-Triassic facies zones in terrane reconstructions in the Alpine-Northern Pannonian domain. *Tectonophysics*, *242*(1–2), 19–40. https://doi.org/10.1016/0040-1951(94)00157-5

Haas, J., Kovács, S., Pelikán, P., Kövér, S., Görög, Á., Ozsvárt, P., et al. (2011). Remnants of the accretionary complex of the Neotethys Ocean in Northern Hungary. *Foldtani Kozlony*, *141*(2), 167–196.

Haas, J., Pelikán, P., Görög, Á., Józsa, S., & Ozsvárt, P. (2013). Stratigraphy, facies and geodynamic settings of Jurassic formations in the Bükk Mountains, North Hungary: Its relations with the other areas of the Neotethyan realm. *Geological Magazine*, *150*(1), 18–49. https://doi.org/10.1017/s0016756812000246

Haas, J., Tardi-Filácz, E., Oravecz-Scheffer, A., & Góczán, F. (1997). Cretaceous intersections in Triassic (?) dolomites at Csővár, North Hungary. *Acta Geologica Hungarica*, *40*, 179–196.

Haines, S. H., & van der Pluijm, B. A. (2008). Clay quantification and Ar-Ar dating of synthetic and natural gouge: Application to the Miocene Sierra Mazatán detachment fault, Sonora, Mexico. *Journal of Structural Geology*, *30*(4), 525–538. https://doi.org/10.1016/j.jsg.2007.11.012

Handy, M. R., Schmid, S. M., Bousquet, R., Kissling, E., & Bernoulli, D. (2010). Reconciling plate-tectonic reconstructions of Alpine Tethys with the geological-geophysical record of spreading and subduction in the Alps. *Earth-Science Reviews*, *102*(3–4), 121–158. https://doi.org/10.1016/j.earscirev.2010.06.002

Handy, R. M., Ustaszewski, K., & Kissling, E. (2015). Reconstructing the Alps-Carpathians-Dinarides as a key to understanding switches in subduction polarity, slab gaps and surface motion. *International Journal of Earth Sciences*, *104*, 1–26. https://doi.org/10.1007/s00531-014-1060-3

Hausegger, S., Kurz, W., Rabitsch, R., Kiechl, E., & Brosch, F.-J. (2010). Analysis of the internal structure of a carbonate damage zone: Implications for the mechanisms of fault breccia formation and fluid flow. *Journal of Structural Geology*, *32*(9), 1349–1362. https://doi.org/10.1016/j.jsg.2009.04.014

Heineke, C., Hetzel, R., Nilius, N. P., Zwingmann, H., Todd, A., Mulch, A., et al. (2019). Detachment faulting in a bivergent core complex constrained by fault gouge dating and low-temperature thermochronology. *Journal of Structural Geology*, *127*, 103865. https://doi.org/10.1016/j.jsg.2019.103865

Hess, J. C., & Lippolt, H. J. (1994). Compilation of K-Ar measurements on HDB-1 standard biotite; 1994 Status report. In G. Odin (Ed.), *Phanerozoic time scale, Bulletin de Liaison et d'information* (pp. 19–23). IUGS Subcommision on Geochronology.

Hips, K., & Haas, J. (2006). Calcimicrobial stromatolites at the Permian-Triassic boundary in a western Tethyan section, Bükk Mountains, Hungary. *Sedimentary Geology*, *185*(3–4), 239–253. https://doi.org/10.1016/j.sedgeo.2005.12.016

Hips, K., & Pelikán, P. (2002). Lower Triassic shallow marine succession in the Bükk Mountains, NE Hungary. *Geologica Carpathica*, *53*(6), 1–17.

Hók, J., Schuster, R., Pelech, O., Vojtko, R., & Samajová, L. (2022). Geological significance of Upper Cretaceous sediments in deciphering of the Alpine tectonic evolution at the contact of the Western Carpathians, Eastern Alps and Bohemian Massif. *International Journal of Earth Sciences*, *111*(6), 1805–1822. https://doi.org/10.1007/s00531-022-02201-5

Horváth, F., Bada, G., Szafián, G., Tari, G., Adam, A., & Cloething, S. (2006). Formation and deformation of the Pannonian Basin: Constrains from observational data. *Memoir—Geological Society of London*, *32*(1), 191–206. https://doi.org/10.1144/gsl.mem.2006.032.01.11

Hurford, A. J. (1990). Standardization of fission track dating calibration: Recommendation by the fission track working group of the I.U.G.S. Subcommission on geochronology. *Chemical Geology: Isotope Geoscience section*, *80*(2), 171–178. https://doi.org/10.1016/0168-9622(90)90025-8

Hurford, A. J., & Green, P. F. (1983). The zeta age calibration of fission-track dating. *Chemical Geology*, *41*, 285–317. https://doi.org/10.1016/s0009-2541(83)80026-6

Janák, M., Froitzheim, N., Lupták, B., Vrabec, M., & Krogh Ravna, E. J. (2004). First evidence for ultrahigh pressure metamorphism of eclogites in Pohorje, Slovenia: Tracing deep continental subduction in the Eastern Alps. *Tectonics*, *23*(5), 1–6. https://doi.org/10.1029/2004tc001641

Janák, M., Froitzheim, N., Yoshida, K., Sasinkova, V., Nosko, M., Kobayashi, T., et al. (2015). Diamond in metasedimentary crustal rocks from Pohorje, Eastern Alps: A window to deep continental subduction. *Journal of Metamorphic Geology*, *33*(5), 495–512. https://doi.org/10.1111/jmg.12130

Janák, M., Plašienka, D., Frey, M., Cosca, M., Schmidt, S. T., Lupták, B., & Méres, Š. (2001). Cretaceous evolution of a metamorphic core complex, the Veporic unit, Western Carpathians (Slovakia): P-T conditions and in situ $^{40}Ar/^{39}Ar$ UV laser probe dating of metapelites. *Journal of Metamorphic Geology*, *19*(2), 197–216. https://doi.org/10.1046/j.0263-4929.2000.00304.x

Jeřábek, P., Faryad, S. W., Schulmann, K., Lexa, O., & Tajčmanová, L. (2008). Alpine burial and heterogeneous exhumation of Variscan crust in the west Carpathians: Insight from thermodynamic and argon diffusion modeling. *Journal of the Geological Society, London*, *165*(2), 479–498.

Jia, D., Li, Y., Yan, B., Li, Z., Wang, M., Chen, Z., & Zhang, Y. (2020). The Cenozoic thrusting sequence of the Longmen Shan fold-and-thrust belt, eastern margin of the Tibetan Plateau: Insights from low-temperature thermochronology. *Journal of Asian Earth Sciences*, *198*, 104381. https://doi.org/10.1016/j.jseaes.2020.104381

Juhász, D., Oravecz, É., & Fodor, L. (2021). Two-phase folding in the Nagyvisnyó area, NW Bükk Mts., NE Hungary. In *18th meeting of the central European tectonic studies groups (CETEG)*. 21-25 September, 2021, Terchová, Slovakia, Abstract Book pp. 54.

Kahn, M., Fayon, A. K., & Tikoff, B. (2020). Constraints on the post-orogenic tectonic history along the Salmon River suture zone from low-temperature thermochornology, western Idaho and eastern Oregon. *Rocky Mountain Geology*, *55*(1), 27–54. https://doi.org/10.24872/rmgjournal.55.1.27

Kázmér, M., Dunkl, I., Frisch, W., Kuhlemann, J., & Ozsvárt, P. (2003). The Paleogene forearc basin of the Eastern Alps and Western Carpathians: Subduction erosion and basin evolution. *Journal of the Geological Society*, *160*(3), 413–428. https://doi.org/10.1144/0016-764902-041

Kázmér, M., & Kovács, S. (1985). Permian-Paleogene paleogeography along the eastern part of the Insubric-Periadriatic lineament system: Evidence for continental escape of the Bakony-Drauzug unit. *Acta Geologica Hungarica*, *28*, 71–84.

Koroknai, B. (2004). *Tectono-metamorphic evolution of Paleozoic formations in the Uppony and Szendrő Mts*. PhD dissertation. Eötvös Loránd University.

Koroknai, B., Árkai, P., Horváth, P., & Balogh, K. (2008). Anatomy of a transitional brittle-ductile shear zone developed in a low-T meta-andesite tuff: A microstructural, petrological and geochronological case study from the Bükk Mts. (NE Hungary). *Journal of Structural Geology*, *30*(2), 159–176. https://doi.org/10.1016/j.jsg.2007.10.007

Koroknai, B., Neubauer, F., Genser, J., & Topa, D. (1999). Metamorphic and tectonic evolution of the Austroalpine units at the western margin of the Gurktal Nappe complex, Eastern Alps. *Schweizerische Mineralogische und Petrographische Mitteilungen*, *79*(2), 277–295.

Kovács, S. (1982). Problems of the "Pannonian Median Massif" and the plate tectonic concept. Contributions based on the distribution of Late Paleozoic—Early Mesozoic isopic zones. *Geologische Rundschau*, *71*(2), 617–639. https://doi.org/10.1007/bf01822386

Kovács, S. (1984). North Hungarian Triassic facies types: A review. *Acta Geologica Hungarica*, *27*(3–4), 251–264.

Kovács, S., Haas, J., Szebényi, G., Gulácsi, Z., Pelikán, P., Bagoly-Árgyelán, G., et al. (2008). Permo-Mesozoic formations of the Recsk-Darnó Hill area: Stratigraphy and structure of the pre-Tertiary basement of the Paleogene Recsk orefield. In J. Földessy, & É. Hartai (Eds.), *Recsk and Lahóca geology of the Paleogene ore complex. Geosciences* (pp. 33–56). Miskolc University Press.

Kovács, S., Kozur, H., & Mock, R. (1983). Relations between the Szendrő-Uppony and Bükk Paleozoic in the light of the latest micropaleontological investigations. *Magyar Állami Földtani Intézet Évkönyve 1981 Évről*, 155–175.

Kovács, S., Sudar, M., Grădinaru, E., Gawlick, H.-J., Karamata, S., Haas, J., et al. (2011). Triassic evolution of the tectonostratigraphic units of the Circum-Pannonian region. *Jahrbuch der Geologischen Bundesanstalt*, *151*(3–4), 199–280.

Kovács, Z., Cserkész-Nagy, Á., Gulyás, Á., Güthy, T., Kiss, J., Püspöki, Z., et al. (2020). Mapping of the Salgótarján and Ózd Paleogene subbasins based on seismic and gravity measurement data, and its hydrocarbon geological aspects. *Foldtani Kozlony*, *15*(1), 103–128.

Kralik, M., Klima, K., & Riedmüller, G. (1987). Dating fault gouges. *Nature*, *327*(6120), 315–317. https://doi.org/10.1038/327315a0

Krohe, A. (1987). Kinematics of Cretaceous nappe tectonics in the Austroalpine basement of the Koralpe region (eastern Austria). *Tectonophysics*, *136*(3–4), 171–196. https://doi.org/10.1016/0040-1951(87)90024-2

Less, G., Gulácsi, Z., Kovács, S., Pelikán, P., Pentelényi, L., Rezessy, A., & Sásdi, L. (2002). *Geological map of the Bükk Mountains (1:50 000)*. Geological Institute of Hungary.

Less, G., Kovács, S., Szentpétery, I., Grill, J., Róth, L., Gyuricza, G., et al. (2006). *Geology of the Aggtelek-Rudabánya Mts.—Explanatory book for the geological map of the Aggtelek-Rudabánya Mts*. Hungarian Geological Institute.

Lukács, R., Harangi, S., Gál, P., Szepesi, J., Di Capua, A., Norini, G., et al. (2022). Formal definition and description of lithostratigraphic units related to the Miocene silicic pyroclastic rocks outcropping in Northern Hungary: A revision. *Geologica Carpathica*, *73*(2), 137–158. https://doi.org/10.31577/geolcarp.73.2.3

Lužar-Orberiter, B., Mikes, T., Dunkl, I., Babić, L., & von Eynatten, H. (2012). Provenance of Cretaceous synorogenic sediments from the NW Dinarides (Croatia). *Swiss Journal of Geosciences*, *105*(3), 377–399. https://doi.org/10.1007/s00015-012-0107-3

Madarás, J., Hók, J., Siman, P., Bezák, V., Ledru, P., & Lexa, O. (1996). Extension tectonics and exhumation of crystalline basement of the Veporicum unit (Central Western Carpathians). *Slovak Geological Magazine*, *3*(4), 179–183.

Maffione, M., & van Hinsbergen, D. J. J. (2018). Reconstructing Plate Boundaries in the Jurassic Neo-Tethys from the East and West Vardar ophiolites (Greece and Serbia). *Tectonics*, *37*(3), 858–887. https://doi.org/10.1002/2017tc004790

Maluski, H., Rajlich, P., & Matte, P. (1993). ^{40}Ar-^{39}Ar dating of the inner Carpathian Variscan basement and Alpine mylonitic overprinting. *Tectonophysics*, *223*(3–4), 313–337. https://doi.org/10.1016/0040-1951(93)90143-8

Mancktelow, N., Zwingmann, H., Campani, M., Fügenschuh, B., & Mulch, A. (2015). Timing and conditions of brittle faulting on the Silltal-Brenner fault zone, Eastern Alps (Austria). *Swiss Journal of Geosciences*, *108*(2–3), 305–326. https://doi.org/10.1007/s00015-015-0179-y

Mancktelow, N., Zwingmann, H., & Mulch, A. (2016). Timing and conditions of clay fault gouge formation on the Naxos detachment (Cyclades, Greece). *Tectonics*, *35*(10), 2334–2344. https://doi.org/10.1002/2016tc004251

Márton, E., & Márton, P. (1996). Large scale rotations in North Hungary during the Neogene as indicated by paleomagnetic data. *Special Publication—Geological Society of London*, *105*(1), 153–173. https://doi.org/10.1144/gsl.sp.1996.105.01.15

Márton, E., Pavelić, D., Tomljenović, B., Avanić, R., Pamić, J., & Márton, P. (2002). In the wake of a counterclockwise rotating Adriatic microplate: Neogene paleomagnatic results from northern Croatia. *International Journal of Earth Sciences*, *91*(3), 514–523. https://doi.org/10.1007/s00531-001-0249-4

Matenco, L., & Radivojević, D. (2012). On the formation and evolution of the Pannonian Basin: Constraints derived from the structure of the junction area between the Carpathians and Dinarides. *Tectonics*, *31*(6), 1–31. https://doi.org/10.1029/2012tc003206

McIntosh, R. W. (2014). Morphotectonics of the Bükkium. PhD thesis. University of Debrecen.
Meunier, A., & Velde, B. (2004). *Illite*. Springer Verlag.
Mišik, M. (1979). Jurassic and Cretaceous algae (Dasycladales expected) from the West Carpathians. *Bulletin of the Centres de Recherches Exploration-Production Elf-Aquitaine*, *3*(2), 705–712.
Neubauer, F., Dallmeyer, R. D., Dunkl, I., & Schirnik, D. (1995). Late Cretaceous exhumation of the metamorphic Gleinalm dome, Eastern Alps: Kinematics, cooling history and sedimentary response in a sinistral wrench corridor. *Tectonophysics*, *242*(1–2), 79–98. https://doi.org/10.1016/0040-1951(94)00154-2
Neubauer, F., Genser, J., Kurz, W., & Wang, X. (1999). Exhumation of the Tauern window, Eastern Alps. *Physics and Chemistry of the Earth—Part A: Solid Earth and Geodesy*, *24*(8), 675–680. https://doi.org/10.1016/s1464-1895(99)00098-8
Niwa, M., Shimada, K., Tamura, H., Shibata, K., Sueoka, S., Yasue, K., et al. (2016). Thermal constraints on clay growth in fault gouge and their relationship with fault-zone evolution and hydrothermal alteration: Case study of gouges in the Kojaku Granite, Central Japan. *Clays and Clay Minerals*, *64*(2), 86–107. https://doi.org/10.1346/ccmn.2016.0640202
Nuriel, P., Weinberger, R., Rosenbaum, G., Golding, S. D., Zhao, J., Uysal, T. I., et al. (2012). Timing and mechanism of late-Pleistocene calcite vein formation across the Dead Sea Fault Zone, northern Israel. *Journal of Structural Geology*, *36*, 43–54. https://doi.org/10.1016/j.jsg.2011.12.010
Odin, G. S. (1982). *Numerical dating in stratigraphy*. John Wiley & Sons.
Oravecz, É. (2023). Supporting data for the thermo-tectonic evolution of the Nekézseny Thrust [Dataset]. *Figshare Collection*. https://doi.org/10.6084/m9.figshare.c.6799899
Oren, O., Nuriel, P., Kylander-Clark, A. R. C., & Haviv, I. (2020). Evolution and propagation of an active plate boundary: U-Pb ages of fault related calcite from the Dead Sea transform. *Tectonics*, *39*(8), e2019TC005888. https://doi.org/10.1029/2019tc005888
Ortner, H. (2001). Growing folds and sedimentation of the Gosau Group, Muttekopf, Northern Calcareous Alps, Austria. *International Journal of Earth Sciences*, *90*(3), 727–739. https://doi.org/10.1007/s005310000182
Pamić, J., Tomljenović, B., & Balen, D. (2002). Geodynamic and petrogenetic evolution of Alpine ophiolites from the central and NW Dinarides: An overview. *Lithos*, *65*(1–2), 113–142. https://doi.org/10.1016/s0024-4937(02)00162-7
Pantó, G. (1954). *Mining geological mapping in the Uppony Mountains*. Geological Institute of Hungary.
Pelikán, P., Budai, T., Less, G., Kovács, S., Pentelényi, L., & Sásdi, L. (2005). *Geology of the Bükk Mountains—Explanatory book to the geological map of the Bükk Mountains (1:50 000)*. Geological Institute of Hungary.
Petrik, A., Beke, B., Fodor, L., & Lukács, R. (2016). Cenozoic structural evolution of the southwestern Bükk Mts. and the southern part of the Darnó Deformation Belt (NE Hungary). *Geologica Carpathica*, *67*(1), 83–104. https://doi.org/10.1515/geoca-2016-0005
Pevear, D. R. (1999). Illite and hydrocarbon exploration. *Proceedings of the National Academy of Sciences of the United States of America*, *96*(7), 3440–3446. https://doi.org/10.1073/pnas.96.7.3440
Plašienka, D. (2018). Continuity and episodicity in the Early Alpine tectonic evolution of the western Carpathians: How large-scale processes are expressed by the orogenic architecture and rock record data. *Tectonics*, *37*(7), 1–51. https://doi.org/10.1029/2017tc004779
Plašienka, D., Grecula, P., Putis, M., Kovác, M., & Hovorka, D. (1997). Evolution and structure of the Western Carpathians: An overview. *Mineralia Slovaca*, *1997*, 1–24.
Plašienka, D., & Mikuš, M. (2010). Geologická stavba pieninského a šarišského úseku bradlového pásma medzi Litmanovou a Drienicou na východnom Slovensku. *Mineralia Slovaca*, *42*(2), 155–178.
Plašienka, D., & Soták, J. (2015). Evolution of Upper Cretaceous—Paleogene synorogenic basins in the Pieniny Klippen Belt and adjacent zones (Western Carpathians, Slovakia): Tectonic controls over a growing orogenic wedge. *Annales Societatis Geologorum Poloniae*, *85*(1), 43–76. https://doi.org/10.14241/asgp.2015.005
Pleuger, J., Mancktelow, N., Zwingmann, H., & Manser, M. (2012). K-Ar dating of synkinematic clay gouges from Neoalpine faults of the Central, Western and Eastern Alps. *Tectonophysics*, *550–530*, 1–16. https://doi.org/10.1016/j.tecto.2012.05.001
Quidelleur, X., Gillot, P. Y., Soler, V., & Lefèvre, J. C. (2001). K/Ar dating extended into the last millennium: Application to the youngest effusive episode of the Teide volcano (Spain). *Geophysical Research Letters*, *28*(16), 3067–3070. https://doi.org/10.1029/2000gl012821
Ratschbacher, L., Dingeldey, C., Miller, C., Hacker, B. R., & McWilliams, M. O. (2004). Formation, subduction and exhumation of Penninic oceanic crust in the Eastern Alps: Time constraints from $^{40}Ar/^{39}Ar$ geochronology. *Tectonophysics*, *394*(3–4), 155–170. https://doi.org/10.1016/j.tecto.2004.08.003
Ratschbacher, L., Frisch, W., Neubauer, F., Schmid, S. M., & Neugebauer, J. (1989). Extension in compressional orogenic belts: The Eastern Alps. *Geology*, *17*(5), 404–407. https://doi.org/10.1130/0091-7613(1989)017<0404:eicobt>2.3.co;2
Reiners, P. W., Zhou, Z., Ehlers, T. A., Xu, C., Brandon, M. T., Donelick, R. A., & Nicolescu, S. (2003). Post-orogenic evolution of the Dabie Shan, Eastern China, from (U-Th)/He and fission-track thermochronology). *American Journal of Science*, *303*(6), 489–518. https://doi.org/10.2475/ajs.303.6.489
Sammis, C., King, G., & Biegel, R. (1987). The kinematics of gouge deformation. *Pure and Applied Geophysics*, *125*(5), 777–812. https://doi.org/10.1007/bf00878033
Scheiber, T., Viola, G., van der Lelij, R., Margreth, A., & Schönenberger, J. (2019). Microstructurally-constrained versus bulk fault gouge K-Ar dating. *Journal of Structural Geology*, *127*, 103868. https://doi.org/10.1016/j.jsg.2019.103868
Scherman, B. (2018). Mesozoic deformation of the Szarvaskő and Mónosbél Nappes: Villó and Almár Valleys of the SW Bükk Mts. MSc thesis. Eötvös Loránd University.
Schmid, S. F., Fügenschuh, B., Kissling, E., & Schuster, R. (2004). Tectonic map and overall architecture of the Alpine orogen. *Eclogae Geologicae Helvetiae*, *97*(1), 93–117. https://doi.org/10.1007/s00015-004-1113-x
Schmid, S. M., Bernoulli, D., Fügenschuh, B., Matenco, L., Schefer, S., Schuster, R., et al. (2008). The Alpine-Carpathian-Dinaridic orogenic system: Correlation and evolution of tectonic units. *Swiss Journal of Geosciences*, *101*(1), 139–183. https://doi.org/10.1007/s00015-008-1247-3
Schmid, S. M., Fügenschuh, B., Kounov, A., Matenco, L., Nievergelt, P., Oberhänsli, R., et al. (2020). Tectonic units of the Alpine collision zone between Eastern Alps and western Turkey. *Gondwana Research*, *78*, 308–374. https://doi.org/10.1016/j.gr.2019.07.005
Schréter, Z. (1943). Geology of the Bükk Mountains. *Magyar Állami Földtani Intézet Évi Jelentése 1943 Évről*, 378–411.
Schréter, Z. (1945). Uppony, Dédes és Nekézseny, továbbá Putnok vidékének földtani viszonyai. *Magyar Állami Földtani Intézet Évi Jelentése 1941-42 Évről*, 161–237.
Schréter, Z. (1953). Földtani vizsgálatok Nagyvisnyó vidékén. *Magyar Állami Földtani Intézet Évi Jelentése 1951 Évről*, 157–167.
Schuster, R., Kurz, W., Krenn, K., & Fritz, H. (2013). Introduction to the geology of the Eastern Alps. In W. Kurz, M. R. Handy, S. Favaro, H. Fritz, K. Krenn, & A. Scharf (Eds.), *Field guide book, excursion B1, 11th workshop on Alpine geological studies & 7th IFAA* (Vol. 99, pp. 121–133). Bereichte der Geologischen Bundes-Anstalt Wien.

Sibson, R. H. (1977). Fault rocks and fault mechanisms. *Journal of the Geological Society*, *133*(3), 191–213. https://doi.org/10.1144/gsjgs.133.3.0191

Sieglné Farkas, Á. (1984). Palynostratigraphy of the Upper Cretaceous in the Uppony Mts. *Magyar Állami Földtani Intézet Évi Jelentése 1982 Évről*, 101–111.

Steiger, R. H., & Jäger, E. (1977). Subcommission on geochronology: Convention on the use of decay constants in geo- and cosmochronology. *Earth and Planetary Science Letters*, *36*(3), 359–362. https://doi.org/10.1016/0012-821x(77)90060-7

Stojadinovic, U., Krstekanić, N., Matenco, L., & Bogdanović, T. (2022). Towards resolving Cretaceous to Miocene kinematics of the Adria-Europe contact zone in reconstructions: Inferences from a structural study in a critical Dinarides area. *Terra Nova*, *34*(6), 523–534. https://doi.org/10.1111/ter.12618

Stüwe, K., & Schuster, R. (2010). Initiation of subduction in the Alps: Continent or ocean? *Geology*, *38*(2), 175–178. https://doi.org/10.1130/g30528.1

Suppe, J., Chou, G. T., & Hook, S. C. (1992). Rates of folding and faulting determined from growth strata. In K. R. McClay (Ed.), *Thrust tectonics* (pp. 105–121). Springer.

Szentpétery, I. (1988). Oligocene and lower Miocene formations of the Rudabánya mountains and their neighbourhood. *Magyar Állami Földtani Intézet Évi Jelentése 1986 Évről*, 121–128.

Szoldán, Z. (1990). Middle Triassic magmatic sequences from different tectonic settings in the Bükk Mts. (NE Hungary). *Acta Mineralogica et Petrologica*, *266*, 319–341.

Sztanó, O., & Józsa, S. (1996). Interaction of basin-margin faults and tidal currents on nearshore sedimentary architecture and composition: A case study from the Early Miocene of northern Hungary. *Tectonophysics*, *266*(1–4), 319–341. https://doi.org/10.1016/s0040-1951(96)00196-5

Sztanó, O., & Tari, G. (1993). Early Miocene basin evolution in northern Hungary: Tectonics and eustasy. *Tectonophysics*, *226*(1–4), 485–502. https://doi.org/10.1016/0040-1951(93)90134-6

Tari, G. (1994). Alpine tectonics of the Pannonian Basin. PhD thesis. Rice University.

Tari, G. (1995). Eoalpine (Cretaceous) tectonics in the Alpine-Pannonian transition zone. In F. Horváth, G. Tari, & C. Bokor (Eds.), *Extensional collapse of an Alpine orogene and hydrocarbon prospects in the basement and basin fill of the Western Pannonian Basin*, *Guidebook to Fieldtrip, No. 6., AAPG international conference and exhibition* (pp. 133–155).

Tari, G., Bada, G., Boote, D. R. D., Krézsek, C., Koroknai, B., Kovács, G., et al. (2023). The Pannonian super basin: A brief overview. *AAPG Bulletin*, *107*(8), 1391–1417. https://doi.org/10.1306/02172322098

Tari, G., Horváth, F., & Wein, G. (1995). Palinspatic reconstruction of the Alpine/Carpathian/Pannonian system. In F. Horváth, G. Tari, & C. Bokor (Eds.), *Extensional collapse of the Alpine orogen and hydrocarbon prospects in the basement and basin fill of the western Pannonian Basin*. *Guidebook to fieldtrip, AAPG International Conference and Exhibition* (pp. 119–132).

Tari, G., & Linzer, H.-G. (2018). Austrian versus Hungarian bauxites in an Alpine context: A tribute to Prof. Andrea MINDSZENTY. *Foldtani Kozlony*, *148*(1), 35–44. https://doi.org/10.23928/foldt.kozl.2018.148.1.35

Tavani, S., Storti, F., Lacombe, O., Corradetti, A., Munoz, J. A., & Mazzoli, S. (2015). A review of deformation pattern templates in foreland basin systems and fold-and-thrust belts: Implications for the state of stress in the frontal regions of thrust wedges. *Earth-Science Reviews*, *141*, 82–104. https://doi.org/10.1016/j.earscirev.2014.11.013

Telegdi Roth, K. (1951). Geological aspects of the oil explorations near Bükkszék. *Magyar Allami Foldtani Intezet Evkonyve*, *40*, 1–21.

Thöni, M. (1999). A review of geochronological data from the Eastern Alps, Schweiz. *Mineralogische und Petrographische Mitteilungen*, *79*(1), 209–230.

Tomljenović, B., Csontos, L., Márton, E., & Márton, P. (2008). Tectonic evolution of the northwestern internal Dinarides as constrained by structures and rotation of Medvednica Mountains, North Croatia. *Geological Society of London, Special Publications*, *298*(1), 145–167. https://doi.org/10.1144/sp298.8

Torgersen, E., Viola, G., Zwingmann, H., & Harris, C. (2015). Structural and temporal evolution of a reactivated brittle-ductile fault—Part II: Timing of fault initiation and reactivation by K-Ar dating of synkinematic illite/muscovite. *Earth and Planetary Science Letters*, *410*, 212–224. https://doi.org/10.1016/j.epsl.2014.09.051

Torgersen, E., Viola, G., Zwingmann, H., & Henderson, I. H. C. (2015). Inclined K-Ar illite age spectra in brittle fault gouges: Effects of fault reactivation and wall-rock contamination. *Terra Nova*, *27*(2), 106–113. https://doi.org/10.1111/ter.12136

Tributh, H., & Lagaly, G. (1986). *Aufbereitung und Identifizierung von Boden- und Lagerstättentonen* (Vol. 30, pp. 524–529). GIT Labor-Fachzeitschrift.

Ustaszewski, K., Kounov, A., Schmid, S. M., Schaltegger, U., Krenn, E., Frank, W., & Fügenschuh, B. (2010). Evolution of the Adria-Europe plate boundary in the northern Dinarides, from continent-continent collision to back-arc extension. *Tectonics*, *29*(6), 6017–6050. https://doi.org/10.1029/2010tc002668

Ustaszewski, K., Schmid, S. M., Fügenschuh, B., Tischler, M., Kissling, E., & Spakman, W. (2008). A map-view restoration of the Alpine-Carpathian-Dinaridic system for the Early Miocene. *Swiss Journal of Geosciences*, *1*(S1), 273–294. https://doi.org/10.1007/s00015-008-1288-7

Ustaszewski, K., Schmid, S. M., Lugović, B., Schuster, R., Schaltegger, U., Bernoulli, D., et al. (2009). Late Cretaceous intra-oceanic magmatism in the internal Dinarides (northern Bosnia and Herzegovina): Implications for the collision of the Adriatic and European plates. *Lithos*, *108*(1–4), 106–125. https://doi.org/10.1016/j.lithos.2008.09.010

van der Pluijm, B. A., Hall, C. M., Vrolijk, P. J., Pevear, D. R., & Covey, M. C. (2001). The dating of shallow faults in the Earth's crust. *Nature*, *412*(6843), 172–175. https://doi.org/10.1038/35084053

van Gelder, I. E., Matenco, L., Willingshofer, E., Tomljenović, B., Andriessen, A. M., Ducea, M. N., et al. (2015). The tectonic evolution of a critical segment of the Dinarides-Alps connection: Kinematic and geochronological inferences from the Medvednica Mountains, NE Croatia. *Tectonics*, *34*(9), 1952–1978. https://doi.org/10.1002/2015tc003937

van Hinsbergen, D. J. J., Torsvik, T. H., Schmid, S. M., Matenco, L., Maffione, M., Vissers, R. L. M., et al. (2020). Orogenic architecture of the Mediterranean region and kinematic reconstruction of its tectonic evolution since the Triassic. *Gondwana Research*, *81*, 79–229. https://doi.org/10.1016/j.gr.2019.07.009

Velledits, F. (1999). Anisian terrestrial deposits in the sequences of the Northern Bükk Mts. (Anisian-Ladinian layers of the Alsó-Sebes-víz key-section and Miskolc-10 borehole=Zsófiatorony). *Foldtani Kozlony*, *129*(3), 327–361.

Velledits, F. (2004). Anisian terrestrial sediments in the Bükk Mountains (NE Hungary) and their role in the Triassic rifting of the Vardar-Meliata branch of the Neo-Tethys Ocean. *Rivista Italiana di Paleontologia e Stratigrafia*, *110*(3), 659–679.

Velledits, F. (2006). Evolution of the Bükk Mountains (NE Hungary) during the Middle-Late Triassic asymmetric rifting of the Vardar-Meliata branch of the Neotethys Ocean. *International Journal of Earth Sciences*, *95*(3), 395–412. https://doi.org/10.1007/s00531-005-0041-y

Vergés, J., Marzo, M., & Munoz, J. A. (2002). Growth strata in foreland settings. *Sedimentary Geology*, *146*(1–2), 1–9. https://doi.org/10.1016/s0037-0738(01)00162-2

Vermeesch, P. (2012). On the visualization of detrital age distributions. *Chemical Geology*, *312–313*, 190–194. https://doi.org/10.1016/j.chemgeo.2012.04.021

Viola, G., Scheiber, T., Fredin, O., Zwingmann, H., Margreth, A., & Knies, J. (2016). Deconvoluting complex structural histories archived in brittle fault zones. *Nature Communications*, *7*, 1–10. https://doi.org/10.1038/ncomms13448

Vojtko, R., Králiková, S., Jeřábek, P., Schuster, R., Danišík, M., Fügenschuh, B., et al. (2016). Geochronological evidence for the Alpine tectono-thermal evolution of the Veporic unit (Western Carpathians, Slovakia). *Tectonophysics*, *666*, 48–65. https://doi.org/10.1016/j.tecto.2015.10.014

Vozár, J., Ebner, F., Vozárová, A., Haas, J., Kovács, S., Sudar, M., et al. (2010). *Variscan and Alpine terranes of the Circum-Pannonian region*. Slovak Academy of Sciences. Geological Institue and Comenius University.

Wagreich, M. (1995). Subduction tectonic erosion and Late Cretaceous subsidence along the northern Austroalpine margin (Eastern Alps, Austria). *Tectonophysics*, *242*(1–2), 63–78. https://doi.org/10.1016/0040-1951(94)00151-x

Wagreich, M., & Decker, K. (2001). Sedimentary tectonics and subsidence modelling of the type Upper Cretaceous Gosau basin (Northern Calcareous Alps, Austria). *International Journal of Earth Sciences*, *90*(3), 714–726. https://doi.org/10.1007/s005310000181

Wagreich, M., & Faupl, P. (1994). Paleogeography and geodynamic evolution of the Gosau Group of the Northern Calcareous Alps (Late Cretaceous, Eastern Alps, Austria). *Paleogeography, Paleoclimatology, Paleoecology*, *110*(3–4), 235–254. https://doi.org/10.1016/0031-0182(94)90086-8

Williams, R. T., Mozley, P. S., Sharp, W. D., & Goodwin, L. B. (2019). U-Th dating of syntectonic calcite veins reveals the dynamic nature of fracture cementation and healing in faults. *Geophysical Research Letters*, *46*(12), 12900–12908. https://doi.org/10.1029/2019gl085403

Willingshofer, E., Neubauer, F., & Cloetingh, S. (1999). The significance of Gosau-type basins for the Late Cretaceous tectonic history of the Alpine-Carpathian belt. *Physics and Chemistry of the Earth, Part A*, *24*(8), 687–695. https://doi.org/10.1016/s1464-1895(99)00100-3

Woodcock, N. H., & Mort, K. (2008). Classification of fault breccias and related fault rocks. *Geological Maganize*, *145*(3), 435–440. https://doi.org/10.1017/s0016756808004883

Yamasaki, S., Zwingmann, H., Yamada, K., Tagami, T., & Umeda, K. (2013). Constraining the timing of brittle deformation and faulting in the Toki granite, central Japan. *Chemical Geology*, *351*, 168–174. https://doi.org/10.1016/j.chemgeo.2013.05.005

Zelenka, T., Baksa, C., Balla, Z., Földessy, J., & Földessy-Járányi, K. (1983). The role of the Darnó Line in the basement structure of Northeast Hungary. *Geologica Carpathica*, *34*, 53–69.

Zwingmann, H., & Mancktelow, N. (2004). Timing of Alpine fault gouges. *Earth and Planetary Science Letters*, *223*(3–4), 415–425. https://doi.org/10.1016/j.epsl.2004.04.041

Zwingmann, H., Mancktelow, N., Antognini, M., & Lucchini, R. (2010). Dating of shallow faults: New constraints from the AlpTransit tunnel site (Switzerland). *Geology*, *38*(6), 487–490. https://doi.org/10.1130/g30785.1